Digital Signal Processing 110 (2021) 102912

Contents lists available at ScienceDirect

Digital Signal Processing

www.elsevier.com/locate/dsp

The smooth variable structure filter: A comprehensive review

Mohammad Avzayesh [a], Mamoun Abdel-Hafez [a], M. AlShabi [b,c,*], S.A. Gadsden [c]

[a] Department of Mechanical Engineering, American University of Sharjah, P.O Box 26666, Sharjah, United Arab Emirates
[b] Department of Mechanical & Nuclear Engineering, University of Sharjah, P.O Box 27272, Sharjah, United Arab Emirates
[c] College of Engineering and Physical Sciences, University of Guelph, Guelph, Ontario, Canada

ARTICLE INFO

Article history:
Available online 3 December 2020

Keywords:
Estimation theory
Filtering
Kalman filters
Smooth variable structure filter
Robustness

ABSTRACT

The smooth variable structure filter (SVSF) is a type of sliding mode filter formulated in a predictor-corrector format and has seen significant development over the last 15 years. In this paper, we provide a comprehensive review of the SVSF and its variants. The developments, applications and improvements of the SVSF in terms of robustness and optimality are investigated. In addition, the combination of the SVSF with different filtering strategies is considered in an effort to improve estimation accuracy while maintaining robustness to model uncertainty. State estimation techniques such as the unscented and cubature Kalman filters (UKF & CKF), SVSF, the combination of SVSF with UKF (UK-SVSF), and the combination of CKF with SVSF (CK-SVSF) are applied on a 4-DOF industrial robotic arm. The SVSF state estimation performance is examined under different operating conditions. The results of these filters have been compared based a number of statistics such as the root mean squared error (RMSE) and mean absolute error (MAE), among others. It is shown that the UK-SVSF and CK-SVSF strategies acquire the best performance in the presence of uncertainties.

1. Introduction

State estimation is an important step in the monitoring and control of dynamic systems [1]. To mechanistically estimate the state, system's dynamic and measurement models are required [1–4]. The accuracy of the state estimate is affected by many factors. Among these factors, is the linearity/non-linearity of the system model, the uncertainty in the system's dynamic and measurement models, and the amount of disturbance/noise on the dynamic and measurement models [1–5]. Therefore, the performance of the estimator is enhanced by methods that take into account the possible model non-linearity [5]. Additionally, the estimation accuracy will be enhanced by introducing methods that are robust to both model uncertainty and to dynamics and measurement noise uncertainty [6–8].

For well over 70 years, different filtering methods have been developed and implemented to estimate the states of a system. The two most well-known and studied filters are Wiener and Kalman filters (KF). In 1942, Wiener introduced the Wiener filter based on least square methods to estimate the state of a stochastic process [9,10]. The work was primarily motivated by target tracking problems (e.g., anti-aircraft guns). In the early 1960's, the Kalman filter (KF) was introduced by Rudolph Kalman. The KF and its extensions remain the most popular state estimators due to their optimal, or near-optimal, performance and their computational efficiency.

The KF is formulated as a predictor-corrector method where an estimate is first predicted using the system's dynamic model and then corrected using a gain after the measurements are obtained [11,12]. For linear systems with white noise (zero mean and Gaussian distribution), the KF is a minimum mean square error (MMSE) estimator that provides the optimal state estimate. However, should the linear system not be well-known or experience non-white noise, the KF yields suboptimal results and can become unstable. Extensions of the KF has been developed to handle nonlinearity or robustness issues to modeling uncertainties. The Extended Kalman Filter (EKF) makes use of first-order Taylor series expansions (approximations) to linearize the nonlinearities in the system and measurement models [13]. If the system or measurement models are highly non-linear, the first-order linearization process will likely yield inaccurate or unreliable estimates and may cause the EKF to diverge from the true state trajectory [14].

In 2004, Uhlmann and Julier demonstrated that the EKF can be difficult to implement and tune, and is only suitable for systems that are mildly nonlinear [15]. To avoid these limitations, they introduced the Unscented Kalman filter (UKF) that is based on non-probabilistic terms known as sigma points and the 'unscented' transform. The sigma points are used to approximate integrals of nonlinear expectation functions. The UKF process is similar to

* Corresponding author.
E-mail address: malshabi@sharjah.ac.ae (M. AlShabi).

https://doi.org/10.1016/j.dsp.2020.102912

the KF and EKF, however no linearization is required which makes it an attractive method for highly nonlinear functions [14,15]. In 2009, the Cubature Kalman filter (CKF) was introduced as an improved form of the UKF. The CKF is based on analytical-integration for nonlinear systems. It uses the third-degree spherical capture rule which does not require the calculation of a derivative. It generally improves the performance in terms of estimation accuracy, however the CKF is sensitive to modeling uncertainties and has robustness issues [14,16].

Artificial intelligence methods such as Artificial Neural Networks (ANN), soft computing, fuzzy logic, adaptive neuro-fuzzy inference engine (ANFIS), machine learning, and genetic algorithms have been combined with classical filters to enhance their performance [17–19]. These fusion techniques can be used to increase the overall accuracy, reliability, and stability of the estimation process [20–24]. However, these methods are computationally expensive and require extensive training phases that might not be applicable to the entire operation of the dynamic system.

To improve the performance of KF-based filters, different methods can be implemented to handle a *priori*-unknown, or time-varying, dynamics and measurement noise sequences. These methods can be categorized as denoising techniques [25,26] and noise statistics estimation techniques [27–40]. Denoising techniques, however, may adversely affect the accuracy of the final state estimate. Uncertainty identification using Maximum Likelihood estimation (MLE), known as a non-Bayesian approach, is a classical approach that maximizes the likelihood function with a lack of prior state probability density function (PDF) [1]. On the other hand, the Maximum a Posteriori Probability (MAP) estimate, known as the Bayesian approach, utilizes the *a priori* state information to estimate the noise statistics of the measurement and process noise sequences [1]. Estimation of the unknown, and possibly time-varying, measurement and dynamic noise statistics in the form of mean and covariance substantially enhanced the filters accuracy [27–40]. Unknown measurement noise covariance estimation techniques were proposed in [27–37]. These techniques are classified under covariance matching techniques and probabilistic techniques. Detection and identification of measurement bias is addressed in a probabilistic method in [38–40].

To handle model uncertainty, in 2007, Habibi and his team introduced a new hybrid filter based on sliding mode concepts and variable structure theory [41]. This filter, known as the smooth variable structure filter (SVSF), forces the state estimates to vary within a boundary around the true state trajectory, and has been proven to be more robust to model uncertainty and stable compared with the Kalman Filter. However, the SVSF, as compared to the KF, is a sub-optimal filter as it is not robust to dynamics and measurement noise. Hence, a trade-off existed between robustness to modeling uncertainties and estimation accuracy.

In this paper, we provide a comprehensive review of the SVSF and the developments over the last 15 years. A robotic system is then used to demonstrate the performance of the SVSF and other KF-based strategies. The paper is organized as follows: the developments of the SVSF are discussed in Section 2, different applications are summarized in Section 3, the robotic case study and results are shown in Section 4, and the paper is then concluded in Section 5.

2. Development of the smooth variable structure filter

In this section, the development and the revised form of the SVSF will be explained. In addition, the main applications and improvements of the SVSF in terms of robustness and optimality are investigated. Finally, the combination of the SVSF with other filtering strategies is considered to achieve improved accuracy while being robust to modeling uncertainty.

2.1. Sliding mode observer & sliding mode control

In 1977, Utkin defined the Variable Structure System (VSS) as a system composed from a number of subsystems, each described by one or more differential equations, thus making the complete system discontinuous [42]. To describe VSS, consider a match of tennis. The trajectory of the ball is discontinuous since its direction is changing as it crosses the net (left or right). Variable Structure Control (VSC) is a technique to control the system using a gain that allows the system to remain continuous while still switching about its discontinuous hyperplanes [42]. A special type of VSC, known as Sliding Mode Control (SMC), forces the state of the system to switch within its discontinuous hyperplanes [42]. SMC can be described as the tennis racket that forces the ball to move along the desired trajectory. Utkin, Guldner, and Shi proved that sliding on the surfaces makes the system more robust to uncertainties [43]. However, Spurgeon discovered that, in some applications, it is hard to implement proper switching control due to an infinite frequency of switching which causes the controller to lose invariance [44].

Slotine introduced an extension to VSC and SMC called the Sliding Mode Observer (SMO). He combined the discontinuous component with a Luenberger observer, so that the gain will be more operative to nonlinear systems [44]. At the same time, Walcott developed a new technique which separates the linear and nonlinear to two different systems and introduced the SMO strategy [45]. A number of efforts have been made to improve and apply new SMO strategies such as using the Linear Matrix Inequality and new gain factor techniques to separate nonlinearity and uncertainties [46,47].

In general, SMO is a technique that attempts to approximate the state about the desired trajectory by switching between hyperplanes. However, SMO uses SMC theory to force the estimate to follow the true state trajectory. Other methods have been developed and implemented such as the Walcott and Zak observer, Slotine observer, Tan and Edwards's Observer, observers with linear and discontinuous injection, and discontinuous observers [48–50].

2.2. Variable structure filter

In the early 2000s, the variable structure filter (VSF) was introduced as a model-based strategy that improves the robustness and stability of the KF. VSF is a predictor-corrector estimator, formatted similar to the KF, that uses predicted state estimates and updates them based on measurements and a switching gain. The VSF utilizes hyperplanes that bounds parametric uncertainties and a switching gain that enables a robust estimate of the true state trajectory [51,52].

The linear system model (1) and measurement model (2) are shown below where A is the model matrix, B is the input matrix, w_k is the system model noise, H is the measurement matrix, v_{k+1} is the measurement noise, k is the time index, z is the system measurement, and x is the system state estimate [52]:

$$x_{k+1} = Ax_k + Bu_k + w_k \tag{1}$$

$$z_{k+1} = Hx_{k+1} + v_{k+1} \tag{2}$$

Initializing the state estimate $\hat{x}_{k|k}$ allows for the prediction of the state estimates (3) and measurements (4), as follows:

$$\hat{x}_{k+1|k} = \hat{A}\hat{x}_{k|k} + \hat{B}\hat{u}_K \tag{3}$$

$$\hat{z}_{k+1|k} = \hat{H}\hat{x}_{k+1|k} \tag{4}$$

where, $\hat{x}_{k|k}$ is the estimate of the state at time k given the measurements up to time k, $\hat{A}$ and $\hat{B}$ are the estimated of the model and input matrix respectively, $\hat{x}_{k+1|k}$ is the estimate of the state at time $k+1$ given the measurements up to time k, $\hat{H}$ is the estimated measurement matrix and $\hat{z}_{k+1|k}$ is the estimate of the measurement at time $k+1$ given the measurement at time k. Note that the VSF and all its forms assumed that the measurement matrix shall be known and linear, which means that $\hat{H}=H$. Next, the updated state estimates (5) and measurements (6) are calculated using a correcting gain (K_{VSF}):

$$\hat{x}_{k+1|k+1} = \hat{x}_{k+1|k} + K_{VSF} \tag{5}$$

$$\hat{z}_{k+1|k+1} = H\hat{x}_{k+1|k+1} \tag{6}$$

where, gain factor K_{VSF} is calculated using the following complex function [53]:

$$\begin{aligned} K_{VSF} = \hat{A}^{-1}H^{+}\Bigg[\Bigg(H\hat{A}\Bigg\{&\gamma\left|H^{+}\right||e_{z_{k+1|k}}| \\ &+\left|\hat{A}^{-1}H^{+}\left(HAH^{+}-H\hat{A}H^{+}\right)_{max}z_{k+1}\right| \\ &+\begin{bmatrix} |H^{+}| \\ +|\hat{A}^{-1}H^{+}|\begin{pmatrix}(HAH^{+}-H\hat{A}H^{+})_{max}+ \\ H\hat{A}H^{+}+\mathrm{I}_{m\times m}\end{pmatrix}\end{bmatrix}(\mathrm{V})_{max} \\ &+\left|\hat{A}^{-1}H^{+}(HB-H\hat{B})_{max}u_{k+1}\right| \\ &+\left[\left|\hat{A}^{-1}\right|+\right](W)_{max}\Bigg\}\Bigg)\circ sign(e_{z_{k+1|k}})\Bigg] \end{aligned} \tag{7}$$

where, γ represent the diagonal matrix with $\gamma_{ii}\geq 1$ and $e_{z_{k+1|k}}$ is the predicted innovation error which is calculated as $e_{z_{k+1|k}} = z_{k+1}-\hat{z}_{k+1|k}$. Also, $(.)_{max}$ denotes the upper bound of the inside element, $\circ$ represents element-by-element matrix multiplication and $sign\ (e_{z_{k+1|k}})$ is a vector described as:

$$sign(e_{z_{k+1|k}}) = \left[sign(e_{z_{1_{k+1|k}}})\dots sign(e_{z_{m_{k+1|k}}})\right]^{T} \tag{8}$$

where, $i=1,2,3,\dots,m$ is the ith element in $e_{zi_{k+1|k}}$. It should be noticed that the general form of $sign(e)$ can be described as:

$$sign(e) = \begin{cases} e/|e| & e\neq 0 \\ 0 & e=0 \end{cases} \tag{9}$$

The advantage of VSF compared to SMO is that the noise and uncertainties are better described and have physical representation. However, the VSF is only applicable to linear systems with sub-optimal results. Furthermore, chattering of each state estimate due to the switching gain can lead to improved estimation results in some cases [52]. In an effort to reduce chattering and provide a smoother result, a smoothing boundary layer (Ψ) that utilizes the saturation function instead of a sign function may be used. Note that a trade-off may exist between the width of the boundary layer and the accuracy of the estimates. For this purpose, the width of the VSF boundary layer is often tuned by trial-and-error [52–54]. The boundary layer may be described as follows:

$$\begin{aligned} \psi = \left|\hat{A}^{-1}H^{+}\right|\left|H\hat{A}\right|&\left|\left|\hat{A}^{-1}H^{+}\begin{pmatrix}HAH^{+}- \\ H\hat{A}H^{+}\end{pmatrix}_{max}(z)_{max}\right|\right. \\ &+\begin{bmatrix} |H^{+}| \\ +|\hat{A}^{-1}H^{+}|\begin{pmatrix}(HAH^{+}-H\hat{A}H^{+})_{max}+H\hat{A}H^{+} \\ +\mathrm{I}_{m\times m}\end{pmatrix}\end{bmatrix} \\ &\times(\mathrm{V})_{max}+\left|\hat{A}^{-1}H^{+}(HB-H\hat{B})_{max}(\mathrm{u})_{max}\right| \\ &+\left[\left|\hat{A}^{-1}\right|\right](W)_{max}\left.\right| \end{aligned} \tag{10}$$

2.3. Extended variable structure filter (EVSF)

In 2006, Habibi introduced an extension to VSF to overcome the linearity limitation in the VSF. The EVSF was developed based on an internal model that estimates the predicted estimates and then updates them using a corrector term or gain. Similar to the EKF, it uses the Jacobian method to linearize the nonlinear system and measurement functions [53,55]. The EVSF is formatted similar to the VSF, however it includes a linearization step. Starting with an initial state estimate, $\hat{x}_{k|k}$, the state estimates and measurements may be predicted using the following:

$$\hat{z}_{k+1|k+1} = H\hat{x}_{k+1|k+1} \tag{11}$$

$$\hat{x}_{k+1|k} = \hat{f}(\hat{x}_{k|k},\hat{u}_{K}) \tag{12}$$

$$\hat{z}_{k+1|k} = H\hat{x}_{k+1|k} \tag{13}$$

where, $\hat{f}(\hat{x}_{k|k},\ \hat{u}_{K})$ is the nonlinear system model. The correcting gain factor (K_{EVSF}) is used to update the state estimates and measurements, as per the following:

$$\hat{x}_{k+1|k+1} = \hat{x}_{k+1|k} + K_{EVSF} \tag{14}$$

$$\hat{z}_{k+1|k+1} = H\hat{x}_{k+1|k+1} \tag{15}$$

where, the gain (K_{EVSF}) is defined as:

$$\begin{aligned} K_{EVSF} = \hat{\phi}_{k}^{-1}H^{+}\Big[\Big\{&\left|(H)_{max}\right|\left|(\hat{\phi})_{max}\right|\left[\gamma\left|\left(H^{+}\right)_{max}\right||e_{z_{k+1|k}}|\right. \\ &+\left|\left(\hat{\phi}^{-1}\right)_{max}\right|\left|\left(f(x_{k},u_{k})-\hat{f}(\hat{x}_{k|k},\hat{u}_{K})\right)_{max}\right| \\ &+\begin{bmatrix}|(\hat{\phi}^{-1})_{max}||(H^{+})_{max}|+ \\ (H^{+})_{max}\end{bmatrix}(\mathrm{V})_{max} \\ &+\left.\left|\left(\hat{\phi}^{-1}\right)_{max}\right|(W)_{max}\right]\Big\}\circ sign(e_{z_{k+1|k}})\Big] \end{aligned} \tag{16}$$

where, $\hat{\phi}_{k+1}$ is the updated linearized form around the most recent estimate; $\hat{\phi}_{k+1} = \frac{\partial\hat{f}}{\partial x}\mid_{x=\hat{x}_{k+1|k+1}}$. The main advantage of the EVSF compared to the VSF is that the EVSF is applicable to nonlinear systems. However, linearization is a disadvantage since it reduces the accuracy and reliability of the estimation process.

2.4. Smooth variable structure filter (SVSF)

In 2007, a modified form of the VSF known as the smooth variable structure filter (SVSF) was introduced, Fig. 1. Similar to the previous versions, the SVSF is a predictor-corrector state estimator based on sliding mode concepts and stability theory. The filter is applicable to both linear and nonlinear systems [41,56]. The basic concept of the SVSF is to force the estimates to converge within a boundary of the true state trajectory [54]. Note that the system must be differentiable and observable [41].

For the SVSF, the 'rank' of the system needs to be considered in its implementation. If the system is not fully ranked (number of the independent measurements is less than the number of states), the Luenberger's reduced order method is used to calculate the gain [41,54]. The chattering effect in the SVSF caused by the switching gain has been well studied and used to create new filtering approaches known as the Extended Kalman Smooth Variable Structure Filter (EK-SVSF) and the Unscented Kalman Smooth Variable Structure Filter (UK-SVSF) [57], and will be discussed later in this study.

The SVSF process is summarized as follows for non-linear systems [41]. If the system is linear, the state estimates are predicted using equation (17).

$$\hat{x}_{k+1|k} = \hat{A}\hat{x}_{k|k} + \hat{B}\hat{u}_{K} \tag{17}$$

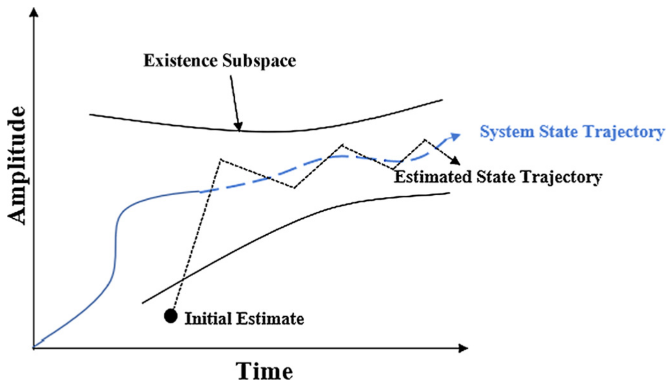

Fig. 1. The smooth variable structure filter, adapted from [56].

where, $\hat{A}$ and $\hat{B}$ are the estimates of the model and input matrix, respectively. If the system is nonlinear, the state estimates are calculated using equation (18). The measurements are then predicted as per equation (19) for non-linear measurements.

$$\hat{x}_{k+1|k} = \hat{f}(\hat{x}_{k|k}, u_K) \tag{18}$$

$$\hat{z}_{k+1|k} = H\hat{x}_{k+1|k} \tag{19}$$

The updated state estimates are found as:

$$\hat{x}_{k+1|k+1} = \hat{x}_{k+1|k} + K_{SVSF} \tag{20}$$

where, the gain K_{SVSF} of the fully ranked measurement can be calculated as follows:

$$K_{SVSF} = H^{+}\left(\gamma|e_{z_{k|k}}| + |e_{z_{k+1|k}}|\right) \circ sign(e_{z_{k+1|k}}) \tag{21}$$

where, $e_{z_{k|k}}$ and $e_{z_{k+1|k}}$ are the previous updated and current predicted measurement error (innovation) respectively, and may be found using the following:

$$e_{z_{k+1|k}} = z_{k+1} - \hat{z}_{k+1|k} \tag{22}$$

$$e_{z_{k|k}} = z_k - \hat{z}_{k|k} \tag{23}$$

Furthermore, note that γ is referred to as the convergence rate and has values between 0 and 1. To reduce the effects of chattering, the sign function is changed to a saturation function [41,51] as per:

$$K_{SVSF} = H^{+}\left(\gamma|e_{z_{k|k}}| + |e_{z_{k+1|k}}|\right) \circ sat(e_{z_{k+1|k}}, \Psi_{k+1}) \tag{24}$$

where, Ψ is the smooth boundary layer width that can be constant or variable and will be explained in more detail later. Also, note that $sat\ (e_{zi_{k+1|k}},\ \Psi_{i_{k+1}})$ for $i = 1, 2, \ldots, n$ is the saturation function that varies between -1 to 1:

$$sat(a, \mathrm{b}) = \begin{Bmatrix} a/\mathrm{b} & |a| \le \mathrm{b} \\ sign(a) & |a| > \mathrm{b} \end{Bmatrix} \tag{25}$$

Note that compared to VSF and EVSF, the SVSF gain is less complex which results in faster convergence and easier implementation. Finally, the updated estimated measurement is found and used to calculate the updated measurement error or innovation:

$$\hat{z}_{k+1|k+1} = H\hat{x}_{k+1|k+1} \tag{26}$$

The SVSF offers two main performance indicators: the first indicator refers to estimation error, and the second indicator is the magnitude of chattering which is inherent to the switching gain. These indicators offer unique applications of the SVSF and have led to a number of developments/improvements [51]:

2.4.1. Robustness & stability improvement

In this section, the stability and robustness of the SVSF is discussed. The first subsection describes the so-called second-order SVSF, the second subsection describes the Predictive Smooth Variable Structure Filter (PSVSF), and the final subsection summarizes the square-root formulation of the SVSF that improves numerical stability.

2.4.1.1. Second-order smooth variable structure filter The Second-Order Smooth Variable Structure Filter (SO-SVSF) is an updated form of the SVSF. It is formulated in a similar manner to the SVSF but makes use of a second-order correction factor. Based on the results described in the literature, it offers improved state estimates in terms of accuracy and is robust to uncertainties [58,59]. The SO-SVSF uses similar equations from (17) to (26), but utilizes a second-order gain. There are two types of second-order gains described. The first one is when the number of measurements (m) equals the number of states (n) which makes H a square matrix, described as:

$$K_{k+1} = H^{+}\left[e_{z_{k+1|k}} - \frac{e_{z_{k|k}}}{2} - \gamma\sqrt{\frac{e_{z_{k|k}} \circ e_{z_{k|k}}}{4} + \frac{\Delta_{z_{k|k}} \circ \Delta_{z_{k|k}}}{2}}\right] \tag{27}$$

where, $\Delta_{z_{k|k}} = e_{z_{k|k}} - e_{z_{k-1|k-1}}$, $\circ$ is the Schur-Product (element-by-element multiplication), and $0 < \gamma < 1$.

For the second case, the number of measurements is less than the number of the states ($m < n$). In this case, the states of the system must be linearized [58,59]. The process is summarized as follows. Consider the following linear system dynamics equation:

$$x_{k+1} = Ax_k + Bu_k + w_k \tag{28}$$

where, x is the state model, A is the state model matrix, u is the input, B is the input matrix (control matrix), and w_k is the process noise at time k. A transformation matrix can be written as follows:

$$Tx_k = \begin{bmatrix} z_{u_k} & z_{l_k} \end{bmatrix}^T \tag{29}$$

where, z_{u_k} is the measurement and z_{l_k} is the artificial measurement. These can be found by partitioning the model, [58] and [59]. The measurement model can be defined as:

$$\begin{bmatrix} z_{k+1} \\ z_{l_{k+1}} \end{bmatrix} = \begin{bmatrix} \Phi_{11} & \Phi_{12} \\ \Phi_{21} & \Phi_{22} \end{bmatrix}\begin{bmatrix} z_k \\ z_{l_k} \end{bmatrix} + \begin{bmatrix} G_1 \\ G_2 \end{bmatrix}u_k + \begin{bmatrix} d_1 \\ d_2 \end{bmatrix}w_k \tag{30}$$

where, $\Phi = T^{-1}AT$, $G = T^{-1}B$, and $d = T^{-1}$. Then, the estimated measurements can be calculated as:

$$\begin{bmatrix} \hat{z}_{k+1} \\ \hat{z}_{l_{k+1}} \end{bmatrix} = \begin{bmatrix} \Phi_{11} & \Phi_{12} \\ \Phi_{21} & \Phi_{22} \end{bmatrix}\begin{bmatrix} \hat{z}_k \\ \hat{z}_{l_k} \end{bmatrix} + \begin{bmatrix} G_1 \\ G_2 \end{bmatrix}u_k \tag{31}$$

Finally, the gain in this case is calculated as:

$$K_{k+1} = \Phi_{22}\Phi_{12}^{-1}\left[\left(e_{z_{k+1|k}} - \frac{e_{z_{k|k}}}{2}\right) - \gamma\sqrt{\frac{e_{z_{k|k}} \circ e_{z_{k|k}}}{4} + \frac{\Delta_{z_{k|k}} \circ \Delta_{z_{k|k}}}{2}}\right] \tag{32}$$

where, $\Delta_{z_{k|k}} = e_{z_{k|k}} - e_{z_{k-1|k-1}}$, $\circ$ is the Schur-Product (element-by-element multiplication), and $0 < \gamma < 1$.

2.4.1.2. Predictive smooth variable structure filter (PSVSF) The Predictive Smooth Variable Structure Filter (PSVSF) is another form of the SVSF. According to the literature, it works better with the existence of errors albeit sub-optimally, [60] and [61]. The PSVSF method is described as per the following:

$$x_{k+1} = f(x_k) + g(x_k)d_k \tag{33}$$

where, f is the differentiable model vector, x is the system model vector, d is the system model error vector, g is the distribution matrix, z is the system measurement vector, h is the differentiable measurement vector, and v is the measurement noise vector which is assumed to be gaussian, zero-mean with covariance equal to R. The state estimates and estimated measurements are defined as:

$$\hat{x}_{k+1} = f(\hat{x}_k) + g(\hat{x}_k)d_k \tag{34}$$

$$\hat{z}_k = h(\hat{x}_k) \tag{35}$$

Next, Lie derivatives can be described as [62]:

$$L_f^m(h_i) = h_i, \quad \text{for } m = 0 \tag{36}$$

$$L_f^m(h_i) = \frac{\partial L_f^{m-1}(h_i)}{\partial x_k} f(x_k), \quad \text{for } m \geq 1 \tag{37}$$

$$L_{g,j} L_f^m(h_i) = \frac{\partial L_f^m(h_i)}{\partial x_k} g_j(x_k) \tag{38}$$

where, g_j is the jth column of $g(x_k)$ and h_i is the ith component of $h(x_k)$. The Taylor series expansion of the measurement can be calculated as:

$$z_{k+1} = z_k + Z[x_k, \Delta k] + \Lambda(\Delta k)U[x_k]d_k + o(e_k + \Delta k) \tag{39}$$

where, Δk is the interval, $o(e_k + \Delta k) = \epsilon[x_k, d_t] + v_{k+1}$, $\epsilon[x_k, d_t]$ is the higher order discretization error and $U[x_k]$ can be defined as:

$$U_{i,j}[x_k] = L_{g,j} L_f^{r_i} h_i[x_k], \; i = 1, 2, \ldots, l \text{ and } j = 1, 2, \ldots, p \tag{40}$$

Also, $\Lambda(\Delta k)$ is the diagonal matrix with the diagonal element λ_{ii} equal to:

$$\lambda_{ii} = \frac{\Delta k^{r_i}}{r_i!}, \quad \text{for } i = 1, 2, \ldots, l \tag{41}$$

and, r_i is the relative degree of the system so that the below condition is applicable:

$$L_g L_f^m h(x) = 0, \quad \text{for } 0 \leq m \leq r - 1 \tag{42}$$

$$L_g L_f^{r-1} h(x) \neq 0 \tag{43}$$

Therefore, the vector $Z[x_k, \Delta k]$ can be calculated as:

$$Z[x_k, \Delta k] = \sum_{c=1}^{r_i} \frac{\Delta k^m}{c!} L_f^c(h_i), \quad \text{for } i = 1, 2, \ldots, l \tag{44}$$

where r_i causes the above equations to be applicable and based on those equations, the measurement equation can be expanded as:

$$z_{k+1} = \hat{z}_k + Z[\hat{x}_k, \Delta k] + \Lambda(\Delta k)U[\hat{x}_k]d_k + o(\hat{e}_k + \Delta k) \tag{45}$$

To simplify this process further, the estimated measurement with modeling uncertainties can be described as:

$$\hat{z}_{k+1} = \hat{z}_k + Z[\hat{x}_k, \Delta k] + \Lambda(\Delta k)U[\hat{x}_k]d_k \tag{46}$$

$$z_{k+1} = o(\hat{e}_k + \Delta k) \tag{47}$$

Finally, the predicted and updated innovation error can be calculated as follows:

$$e_{z_{k+1|k}} = z_{k+1} - \hat{z}_k - Z[\hat{x}_k, \Delta k] \tag{48}$$

$$e_{z_k} = z_k - \hat{z}_k \tag{49}$$

From (32) to (46), the system model error vector d_k can be defined as:

$$d_k = \left\{\Lambda(\Delta k)U[\hat{x}_k]\right\}^{+}\left(\gamma |e_{z_k}| + |e_{z_{k+1|k}}|\right) \circ sign(e_{z_{k+1|k}}) \tag{50}$$

where, the convergence rate γ is the diagonal matrix with $0 < \gamma_{ii} < 1$ and $sign(e_{z_{k+1|k}})$ can be calculated from equation (9).

2.4.1.3. Square-root smooth variable structure filter (SR-SVSF) The Square-Root SVSF (SR-SVSF) is based on the Square-Root formulation of the KF which was introduced by the Potter and Andrews [63]. It is based on the assumption of the availability of the square root of state error covariance P where $P = BB^T$ and B is the square-root covariance matrix. The filter is introduced with the aim of improving numerical robustness and stability [64].

The predicted state estimate and its square root covariance can be described as:

$$\hat{x}_{k+1|k} = F(\hat{x}_{k|k}, \hat{u}_K) \tag{51}$$

$$B_{k+1|k} B_{k+1|k}^T = F B_{k|k} B_{k|k}^T F_k^T + Q_k^{\frac{1}{2}} Q_k^{\frac{T}{2}} \tag{52}$$

where, $F(\hat{x}_{k|k}, \; \hat{u}_K)$ is the nonlinear form of the system model description, Q is the system noise covariance matrix, and H is the measurement matrix. The measurement prediction can be described as:

$$\hat{z}_{k+1|k} = H\hat{x}_{k+1|k} \tag{53}$$

Then the innovation error can be found as per the following:

$$e_{z_{k+1|k}} = z_{k+1} - \hat{z}_{k+1|k} \tag{54}$$

The SVSF gain can be calculated based on equation (24). Then, the updated square-root covariance matrix can be found as follows:

$$B_{k+1|k+1} = B_{k+1|k}\left(I - a\gamma\beta\beta^T\right) \tag{55}$$

where, $a = (\beta^T\beta + R_{i,k+1})^{-1}$, $\beta = B_{k+1|k}^T H^T$ and $\gamma = (1 + \sqrt{aR_{i,k+1}})$. Finally, the updated measurement estimate, and the posteriori innovation error can be calculated as follows:

$$\hat{z}_{k+1|k+1} = H\hat{x}_{k+1|k+1} \tag{56}$$

$$e_{z_{k+1|k+1}} = z_{k+1} - \hat{z}_{k+1|k+1} \tag{57}$$

2.4.2. Optimality improvement

The performance of the SVSF can be improved by considering the optimality of the filter. SVSF optimality can be enhanced by calculating an optimal time-varying smoothing boundary layer (Ψ) [53]. In the standard SVSF introduced by Habibi, a constant and typically large boundary layer width causes the filter to lose accuracy. However, if the smoothing boundary layer width is too small, the filter will not smooth the noise. A trade-off exists between the two.

Figs. 2 and 3 describe the effect of the smoothing boundary layer on the state estimates. The existence subspace (β) represents the amount of uncertainties in the system (e.g., noise, modeling error, and so forth). The SVSF forces the estimates to chatter back-and-forth about the true state trajectory within the boundary layer. If the switching is of high frequency, chattering will occur which is generally undesirable. The existence subspace (β) or the constant smooth boundary layer (Ψ_{fixed}) is the $m \times m$ diagonal matrix with off-diagonal elements equal to zero. In general, the diagonal elements can be found by trial and error based on the design criteria [54].

$$\Psi_{fixed} = \begin{bmatrix} \Psi_1 & \cdots & 0 \\ \vdots & \ddots & \vdots \\ 0 & \cdots & \Psi_m \end{bmatrix} \tag{58}$$

where, m is the number of measurements.

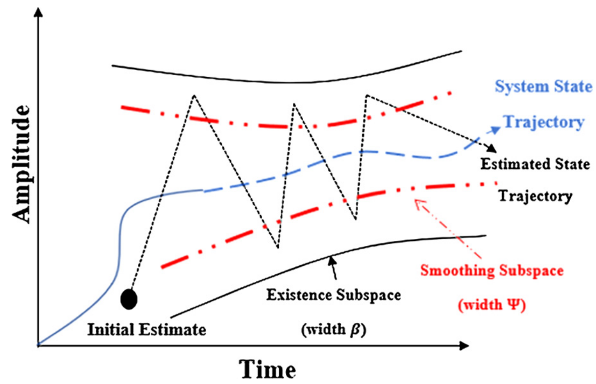

Fig. 2. Presence of chattering effect $\beta > \Psi$, adapted from [11] and [54].

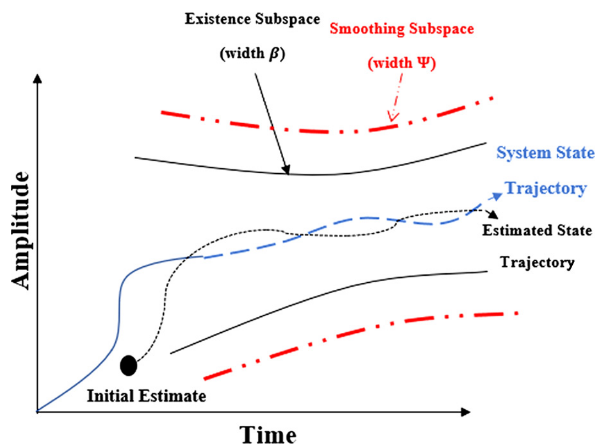

Fig. 3. Smoothed estimated trajectory $\beta < \Psi$, adapted from [11] and [54].

Gadsden introduced a time-varying smoothing boundary layer (Ψ_{VBL}) which greatly improved the performance of the SVSF [54]. If the defined Ψ_{VBL} is greater than the Ψ_{fixed}, the chattering effect will be minimized, and the system will be smoother. However, if the Ψ_{fixed} is larger than the Ψ_{VBL}, the effect of chattering will remain due to the existence of the uncertainties in the system [65]. The chattering effect can be used to combine the SVSF with different filtering strategies which will be explained later.

Gadsden developed an equation to calculate the time-varying boundary layer as a function of *a priori* and a posteriori innovation error ($e_{z_{k|k}}, e_{z_{k+1|k}}$), memory or converges rate (γ), linearized measurement matrix (H), posteriori state estimate covariance ($P_{k+1|k}$) and innovation covariance (S_{k+1}) which can be described as [53,54,66]:

$$\Psi_{VBL}^{-1} = diag(A)^{+} H P_{k+1|k} H^{T} S_{k+1}^{-1} \tag{59}$$

$$\Psi_{VBL} = \begin{bmatrix} \Psi_{11} & \cdots & \Psi_{1m} \\ \vdots & \ddots & \vdots \\ \Psi_{m1} & \cdots & \Psi_{mm} \end{bmatrix} \tag{60}$$

where, $A = (|e_{z_{k+1|k}}| + \gamma |e_{z_{k|k}}|)$.

At the same time, Al-Shabi described the time varying boundary layer as a diagonal matrix in general as [51,67]:

$$\begin{aligned} diag(\Psi_{VBL}) = {} & diag\left(|e_{z,1_{k+1|k}}|\right)\left(P_{zz1,k+1|k} \circ I_{n\times n}\right) \\ & \times \left(P_{zz1,k+1|k} \circ I_{n\times n} - R_{k+1} \circ I_{n\times n}\right)^{-1} \end{aligned} \tag{61}$$

where, P_{zz} is the measurement covariance, I is the identity matrix, and R is the measurement noise covariance.

Another form of the SVSF was introduced in [68]. The authors presented a modified form of the boundary layer without losing the stability of the filter [69].

$$\Psi_{k+1} = (P_{k+1|k} + R_{k+1}) P_{k+1|k}^{-1}\left(|e_{z_{k+1|k}}| + \gamma |e_{z_{k|k}}|\right) \tag{62}$$

where, R is the measurement covariance, and $P_{k+1|k}$ is the state covariance matrix that can be calculated as:

$$P_{k+1|k} = A P_{k|k} A^{T} + Q_k \tag{63}$$

where, A is the linear system matrix, and Q is the system noise covariance matrix.

Another method was implemented to create the partitioned time-varying smoothing boundary layer which has both upper bound and lower bounds [70]. It can be described as per equations (64) and (65).

$$\Psi_u = diag\left(|e_{z_{k+1|k}}| + \gamma |e_{z_{k|k}}|\right)^{-1} H P_{k+1|k} H^{T} S_{k+1}^{-1} \tag{64}$$

where, subscript u represent the upper bound and it is a function of *a priori* and a posteriori innovation error ($e_{z_{k+1|k}}$, $e_{z_{k|k}}$), memory or converges rate (γ), linearized measurement matrix (H), *a priori* state estimate covariance ($P_{k+1|k}$) and innovation covariance (S_{k+1}). The lower-bound is calculated as:

$$\Psi_l = \left|\Phi_{22}\Phi_{12}^{-1} e_{z_{k+1|k}}\right| + \gamma \left|\Phi_{12}^{-1} e_{z_{k|k}}\right| \tag{65}$$

where, subscript l represent the lower bound and Φ can be calculated as $\Phi = T^{-1} A T$, and T can be calculated based on equation (29). Note that the optimality is achieved by having a good knowledge to the system. If it is not well defined, the proposed filters give their original solutions, which are involved with robustness and stability.

2.4.3. Combination of SVSF with other filtering strategies

The SVSF has been combined with a number of different filtering strategies to create new filters that maintain the robustness of the SVSF while benefiting from the accuracy of the other filters (e.g., KF for linear systems). There are two main methods for combining the SVSF with other strategies: the first involves the chattering function created by Al-Shabi, and the second involves the use of the time-varying boundary layer created by Gadsden [54,57]. The SVSF has been successfully combined with the KF, EKF, UKF, CKF, PF, among other filters [54,56,57].

In 2008, Habibi combined the EKF and SVSF and created the Extended Kalman Smooth Variable Structure Filter (EK-SVSF). He used the EKF gain factor ($K_{EKF,k+1}$) and its innovation error $e_{z_{k+1|k}}$ to calculate the saturation function in the SVSF gain as per the following [71]:

$$\begin{aligned} K_{SVSF,k+1} = {} & H^{+}\left(\gamma |e_{z_{k|k}}| + |e_{z_{k+1|k}}| + |\Pi|\right) \\ & \circ\, sat(K_{EKF,k+1} e_{z_{k+1|k}}, 1) \end{aligned} \tag{66}$$

where, Π is the constant positive vector with element $\Pi_i < 1$ and:

$$K_{EKF,k+1} = P_{k+1|k} H_{k+1}' S_{k+1}' \tag{67}$$

where, $P_{k+1|k}$ is the predicted state error covariance, H_{k+1} is the linearized model matrix, and S_{k+1} is the innovation (residual) covariance.

Gadsden developed a new method by using the time-varying smoothing boundary layer (Ψ_{VBL}) to combine a number of different filters [54]. The main difference between the SVSF and KF extensions is the calculation of the gain.

As described in Fig. 4, the value of the smoothing boundary layer (fixed vs time-varying) is used to indicate which gain should

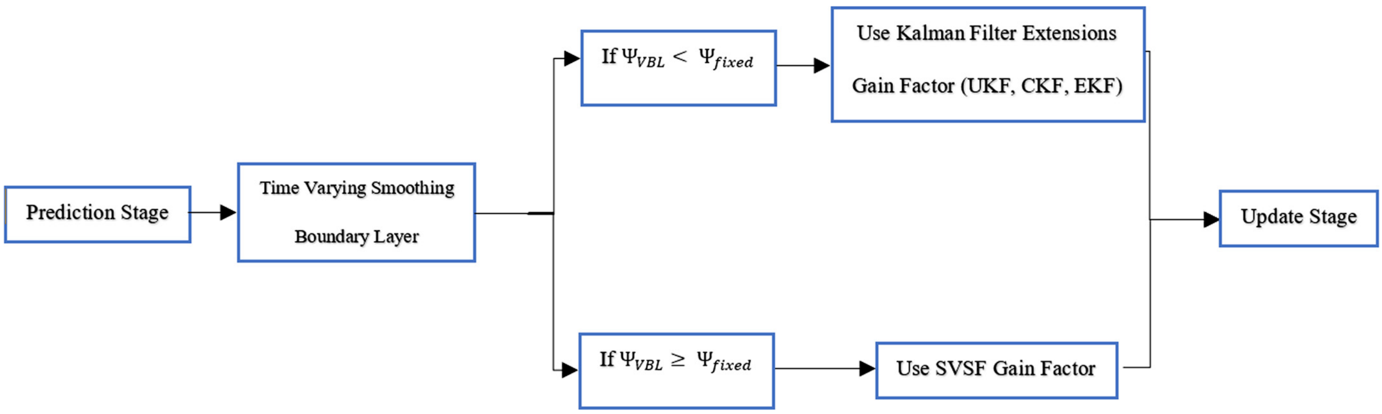

Fig. 4. Methodology for combining the SVSF with other estimation strategies, adapted from [11].

be implemented (e.g., SVSF or KF). If the $\Psi_{VBL} < \Psi_{fixed}$, then the strategy uses the KF gain to maintain optimality. If $\Psi_{VBL} \geq \Psi_{fixed}$, the SVSF gain is used to maintain robustness at the cost of estimation accuracy [11,65].

Around the same time, Al-Shabi used the SVSF chattering signal to combine filtering strategies. Initially, two SVSF formulas, (21) and (24), were used. Later, the gain in equation (24) was replaced with other KF gains such as the EKF and UKF [51].

2.4.3.1. Extended Kalman smooth variable structure filter (EK-SVSF) The combination of the EKF and SVSF is referred to as the EK-SVSF [54]. The EK-SVSF equations is summarized in this section [11].

First, the state estimates, covariance, and measurements are predicted (based on initial values or the previous step):

$$\hat{x}_{k+1|k} = F(\hat{x}_{k|k}, \hat{u}_K) \tag{68}$$

$$P_{k+1|k} = F_k P_{(k|k)} F_k^T + Q_{k+1} \tag{69}$$

$$\hat{z}_{k+1|k} = \hat{H}\hat{x}_{k+1|k} \tag{70}$$

where, $F(\hat{x}_{k|k},\ \hat{u}_K)$ is the nonlinear form of the system model, Q is the system noise covariance matrix, and H is the linearized measurement matrix. Next, the innovation and its covariance are found as per the following:

$$e_{z_{k+1|k}} = z_{k+1} - \hat{z}_{k+1|k} \tag{71}$$

$$S_{k+1} = H_{k+1} P_{k+1|k} H_{k+1}^{-1} + R_{k+1} \tag{72}$$

where, R is the measurement noise covariance matrix.

Based on equation (59), the time-varying smoothing boundary layer is calculated and compared to the fixed smoothing boundary layer. Subsequently, the appropriate gain (EKF or SVSF) is selected and used. If the $\Psi_{VBL} < \Psi_{fixed}$, use the EKF gain to update the state estimates:

$$K_{EKF,k+1} = P_{k+1|k} H'_{k+1} S'_{k+1} \tag{73}$$

where, $P_{k+1|k}$ is the state prediction covariance, H_{k+1} is the linearized model matrix, and S_{k+1} is the innovation (residual) covariance. However, if the time-varying boundary layer width is larger than the fixed boundary layer ($\Psi_{VBL} \geq \Psi_{fixed}$), the SVSF gain as per (24) must be used to maintain robustness. The state estimates and covariance can then be updated as:

$$\hat{x}_{k+1|k+1} = \hat{x}_{k+1|k} + K_{k+1} e_{z_{k+1|k}} \tag{74}$$

$$P_{k+1|k+1} = (I - K_{k+1}H) P_{k+1|k} \begin{pmatrix} I- \\ K_{k+1}H \end{pmatrix}^T + K_{k+1} R_{k+1} K_{k+1}^T \tag{75}$$

Finally, the updated estimated measurement, and the updated measurement error are found and used in the next time step:

$$\hat{z}_{k+1|k+1} = \hat{H}\hat{x}_{k+1|k+1} \tag{76}$$

$$e_{z_{k+1|k}} = z_{k+1} - \hat{z}_{k+1|k+1} \tag{77}$$

2.4.3.2. Unscented Kalman smooth variable structure filter (UK-SVSF) As described earlier, the Unscented Kalman Filter (UKF) is an alternative to the EKF which uses sigma points to estimate the states. It is more complex than EKF since it uses $2n+1$ sigma points [72]. The combination of UKF and SVSF is known as UK-SVSF and the process can be described as follows [11]. First, the sigma points and corresponding weights are initialized:

$$X_{0,k|k} = \hat{x}_{k|k} \tag{78}$$

$$W_0 = \frac{k}{n+k} \tag{79}$$

where, k is a design value (usually less than 1). The next n number of sigma points and the corresponding weights can be calculated as [72]:

$$X_{i,k|k} = \hat{x}_{k|k} + \left(\sqrt{(n+k)P_{k|k}}\right)_i \tag{80}$$

$$W_i = \frac{1}{2(n+k)} \tag{81}$$

The rest of the n number of sigma points and their corresponding weights can be calculated as:

$$X_{i+n,k|k} = \hat{x}_{k|k} - \left(\sqrt{(n+k)P_{k|k}}\right)_i \tag{82}$$

$$W_{i+n} = \frac{1}{2(n+k)} \tag{83}$$

where, $(\sqrt{(n+k)P_{k|k}})_i$ is the ith row or column corresponding to the square root of $(n+k)P_{k|k}$. Sigma points propagation calculation can be described as:

$$\hat{X}_{i,k+1|k} = F(X_{i,k|k}, u_k) \tag{84}$$

State estimate and its corresponding error covariance prediction are then calculated as:

$$\hat{x}_{k+1|k} = \sum_{i=0}^{2n} W_i \hat{X}_{i,k+1|k} \tag{85}$$

$$P_{xx,k+1|k} = \sum_{i=0}^{2n} W_i \begin{pmatrix} \hat{X}_{i,k+1|k}- \\ \hat{x}_{k+1|k} \end{pmatrix} \begin{pmatrix} \hat{X}_{i,k+1|k}- \\ \hat{x}_{k+1|k} \end{pmatrix}^T \tag{86}$$

The nonlinear measurement propagation can be described as:

$$\hat{Z}_{i,k+1|k} = h(\hat{X}_{i,k+1|k}, u_k) \tag{87}$$

where, h is the measurement matrix. The predicted measurement and its corresponding covariance can be calculated as:

$$\hat{z}_{k+1|k} = \sum_{i=0}^{2n} W_i \hat{Z}_{i,k+1|k} \tag{88}$$

$$P_{zz,k+1|k} = \sum_{i=0}^{2n} W_i \begin{pmatrix} \hat{Z}_{i,k+1|k} - \\ \hat{z}_{k+1|k} \end{pmatrix} \begin{pmatrix} \hat{Z}_{i,k+1|k} - \\ \hat{z}_{k+1|k} \end{pmatrix}^T \tag{89}$$

The innovation error is found, similar to previous discussion, as follows:

$$e_{z_{k+1|k}} = z_{k+1} - \hat{z}_{k+1|k} \tag{90}$$

The cross-covariance between measurement and state estimate can be calculated as:

$$P_{xz,k+1|k} = \sum_{i=0}^{2n} W_i \begin{pmatrix} \hat{X}_{i,k+1|k} - \\ \hat{x}_{k+1|k} \end{pmatrix} \begin{pmatrix} \hat{Z}_{i,k+1|k} - \\ \hat{z}_{k+1|k} \end{pmatrix}^T \tag{91}$$

Next, similar to the EK-SVSF strategy, if the $\Psi_{VBL} < \Psi_{fixed}$, then the UKF gain factor is used as:

$$K_{UKF,k+1} = P_{xz,k+1|k} P_{zz,k+1|k}^{-1} \tag{92}$$

Finally, the state estimates and covariance are updated:

$$e_{z_{k+1|k}} = z_{k+1} - \hat{z}_{k+1|k} \tag{93}$$

$$\hat{x}_{k+1|k+1} = \hat{x}_{k+1|k} + e_{z_{k+1|k}} K_{UKF,k+1} \tag{94}$$

$$P_{k+1|k+1} = P_{xx,k+1|k} - K_{UKF,k+1} P_{zz,k+1|k} K_{UKF,k+1}^T \tag{95}$$

However, if the time-varying boundary layer width is larger than the fixed boundary layer ($\Psi_{VBL} \geq \Psi_{fixed}$), the SVSF gain must be used based on (24).

2.4.3.3. Cubature Kalman smooth variable structure filter (CK-SVSF) Cubature Kalman Filter (CKF) is an updated form of the UKF which uses cubature points ζ_i to estimate the nonlinear model state estimation [73–75]. The sigma points ζ_i can be found as per the following:

$$\zeta_i = \begin{Bmatrix} \sqrt{nh_i} & i = 1, 2, \ldots, n \\ -\sqrt{nh_{i-n}} & i = n+1, n+2, \ldots, 2n \end{Bmatrix} \tag{96}$$

where, h_i is the ith elementary column vector [73]. Next the cubature points are initialized as a function of the state estimate $\hat{x}_{k|k}$, its covariance $P_{k|k}$ and cubature points ζ_i as:

$$X_{i,k|k} = \hat{x}_{k|k} + \sqrt{P_{xx,k|k}}\zeta_i, \quad \text{for } i = 1, 2, \ldots, 2n \tag{97}$$

Then, the cubature points are propagated through the nonlinear system function as:

$$X_{i,k+1|k}^* = F(X_{i,k|k}, u_k), \quad \text{for } i = 1, 2, \ldots, 2n \tag{98}$$

The state estimates and error covariance are predicted as per the following two equations:

$$\hat{x}_{k+1|k} = \frac{1}{2n} \sum_{i=0}^{2n} X_{i,k+1|k}^* \tag{99}$$

$$P_{xx,k+1|k} = \frac{1}{2n} \sum_{i=0}^{2n} X_{i,k+1|k}^* X_{i,k+1|k}^{*T} - \hat{x}_{k+1|k}\hat{x}_{k+1|k}^T + Q_{k+1} \tag{100}$$

where, Q_{k+1} is the system noise covariance matrix. The predicted cubature points can be described as:

$$X_{i,k+1|k} = \hat{x}_{k+1|k} + \sqrt{P_{xx,k+1|k}}\zeta_i, \quad i = 1, 2, \ldots, 2n \tag{101}$$

Then, the propagated measurement, predicted measurement and its corresponding covariance matrix can be calculated as:

$$Z_{i,k+1|k} = H(X_{i,k+1|k}, u_k) \quad \text{for } i = 1, 2, \ldots, 2n \tag{102}$$

$$\hat{z}_{k+1|k} = \frac{1}{2n} \sum_{i=0}^{2n} Z_{i,k+1|k} \tag{103}$$

$$P_{zz,k+1|k} = \frac{1}{2n} \sum_{i=0}^{2n} Z_{i,k+1|k} Z_{i,k+1|k}^T - \hat{z}_{k+1|k}\hat{z}_{k+1|k}^T + R_{k+1} \tag{104}$$

where, R_{k+1} is the measurement noise covariance. Next, the cross-covariance of the states and measurements are calculated:

$$P_{xz,k+1|k} = \frac{1}{2n} \sum_{i=0}^{2n} X_{i,k+1|k} Z_{i,k+1|k}^T - \hat{x}_{k+1|k}\hat{z}_{k+1|k}^T \tag{105}$$

Similar to the EK-SVSF and UK-SVSF, if $\Psi_{VBL} < \Psi_{fixed}$, the CKF gain factor is used:

$$K_{CKF,k+1} = P_{xz,k+1|k} P_{zz,k+1|k}^{-1} \tag{106}$$

If the time-varying boundary layer width is larger, than the fixed boundary layer ($\Psi_{VBL} \geq \Psi_{fixed}$), the SVSF gain (24) must be used to maintain robustness.

2.4.4. Fuzzy smooth variable structure filter (Fuzzy-SVSF)

In 1965, Zadeh introduced a method in human approximate reasoning known as fuzzy logic. Fuzzy logic is a set of mathematical principles that represent the knowledge based on a degree of membership functions [76]. Fuzzy Logic is based on IF-Then rules to approximate the performance of the system. A new approach to combine fuzzy logic with KF was proposed in [77]. In this study, a revised form of the KF [77] was used. In [78], fuzzy logic was combined with the SVSF, and the strategy is referred to as Fuzzy-SVSF. The formulation of Fuzzy-SVSF can be described as per the following equations [78]:

$$k_{k+1} = AK_{SVSF} \tag{107}$$

where, A is the system matrix and K_{SVSF} is the SVSF gain. The gain can be calculated based on equation (24). The predicted and updated state estimates are found using equations (108) and (109).

$$\hat{x}_{k+1|k} = A\hat{x}_{k|k} + k_{k+1}e_{z_{k+1|k}} \tag{108}$$

$$\hat{x}_{k+1|k+1} = \hat{x}_{k+1|k} + Bu_{k+1} \tag{109}$$

where, B is the input gain matrix. Then, the fuzzy logic residual ω can be calculated as:

$$\omega_{k+1} = k_{k+1} P_{1,k+1} k_{k+1}^T \tag{110}$$

where, P is the state error covariance matrix calculated using the following two equations:

$$P_{2,k+1} = (A - k_{k+1}H)P_{2,k}A^T + \omega_{k+1} \tag{111}$$

$$P_{1,k+1} = HP_{2,k+1}H^T + \varphi_{k+1} \tag{112}$$

H is the measurement matrix, and φ is the probability density function of measurement error.

3. Applications of the SVSF

This section describes the use of the SVSF and its variants in different applications such as fault detection, positioning and navigation system, target tracking, among many others.

Engineering systems are becoming increasingly complex and dictating the need to maintain robustness to uncertainties and unknown disturbances. Detecting faults and predicting failure are some of the most important features of a system that should be considered for reliability. The combination of Artificial Neural Networks (ANNs) with the SVSF was proposed for the successful fault detection of automotive internal combustion engines [79]. The proposed method demonstrated stability and improved fault diagnosis accuracy compared to Back Propagation (BP), the Levenberg-Marquardt (LM), the Quasi-Newton (QN), and the Extended Kalman Filter (EKF) [79,80]. The combination of the interacting multiple model (IMM) with the SVSF known as IMM-SVSF was applied to an experimental electro-hydrostatic actuator (EHA) [81]. The results were compared with the IMM-EKF, and it was found that the IMM-SVSF had lower false detection rates compared to the IMM-EKF [58,81–83]. The second-order SVSF was also applied on the EHA, and the results demonstrated relatively good tracking accuracy without the loss of stability [84].

In the area of autonomous vehicles, a number of different methods have been implemented to perform self-localization and target tracking. Simultaneous Localization and Mapping (SLAM) is a technique which allows the robot to build a map of the environment and keep track of this map to reach the desired point. SLAM is an interesting as well as difficult technique to study, as the robot location must be estimated in conjunction with the environment. To improve this process, the SVSF was combined with SLAM to introduce the SVSF-SLAM strategy. This method was applied to unmanned ground vehicles (UGVs) and Autonomous Underwater Vehicle (AUV). The results further demonstrated that the SVSF-SLAM and its adaptive form are more robust and accurate compared to the EKF-SLAM [85–90]. Furthermore, the SVSF has been applied on a FastSLAM application [91]. FastSLAM is an alternative solution for SLAM which reduces the quadratic computational complexity and single-hypothesis data association problem of the traditional SLAM. However, FastSLAM is less accurate compared to the traditional method since it ignores the correlation information of the landmarks. To solve this problem, SVSF-FastSLAM was introduced as it is adopted to estimate the position of the landmarks. The result reveals that the proposed method has better accuracy in estimation of the environment and trajectory compared to the FastSLAM. In [92], the SVSF was combined with the quaternion-based error state Kalman Filter (ESKF) to overcome the uncertainty injected in Inertial Measurement Unit (IMU)-based attitude estimation. To validate the ESKF-SVSF algorithm, experimental data collected from Unmanned Aerial Vehicle (UAV). The result demonstrates that the ESKF-SVSF is more accurate in attitude estimation compared to ESKF due to its hybrid formulation, which has the optimality of the ESKF and robustness of SVSF to model uncertainties. Following, a modified form of the SVSF was applied on a 2-D radar tracking application [93]. In this study, the traditional saturation function appears in the formulation of SVSF was replaced with a hyperbolic tangent function. The proposed method, which is referred to Tanh-SVSF, appears to have a better performance as it reduces the chattering effect in the traditional SVSF without adding any computational complexity, while having better accuracy in target tracking compared to the traditional method.

Another approach where information from the joint probabilistic data association (JPDA) is combined with the generalized variable boundary layer (GVBL) and the SVSF to introduce the JPDA-GVBL-SVSF. This method was used for multiple target tracking in clutter [94,95]. Similarly, the SVSF applied to single and multi-target tracking problems were studied and the results compared to the regular filters such as EKF and UKF [96,97]. In 2017, the second-order smooth variable structure filter (SO-SVSF) was integrated with the Strapdown Inertial Navigation System (SINS) [98]. The filter yielded a more robust and precise estimation of the large azimuth misalignment angle [98]. An integrated method that combined the Gaussian Sum Filter (GSF), EKF, and SVSF in a proposed GS-EK-SVSF filter yielded better state estimation accuracy and reliability in target tracking compared with the standard GS-EKF and GS-SVSF [99]. Additionally, a two-pass SVSF-based strategy was implemented on an aerospace actuator [100,101]. The results were compared with KF-based strategies and demonstrated that the SVSF-based method remained stable with high-estimation accuracy compared to the KF-based strategy [100,101].

Other applications of the SVSF include estimation of battery parameters and robotic manipulators. The SVSF has been used to estimate the state of charge (SOC) and state of health (SOH) of lithium-ion (Li-ion) and lithium-polymer (Li-po) batteries [102–104]. Again, the SVSF demonstrated improvements in accuracy and robustness when compared with the EKF method [102–104]. In [105], the SVSF was combined with adaptive SMC to estimate the new operational scheme for multi-level inverters in microgrid. The SVSF was used to estimate the voltage harmonic and voltage unbalance. The results demonstrated that the proposed method optimized the voltage and power required in varying loads. Furthermore, the SVSF was applied on an optimized first-order equivalent circuit-based model (OCV-R-RC) battery over the period of 12 months using real-world varying environments. The experimental results demonstrate the efficiency of the SVSF in the estimation of the state of charge based on the optimized model [106]. In [107], the SVSF was used to estimate the states of a triple-rotary

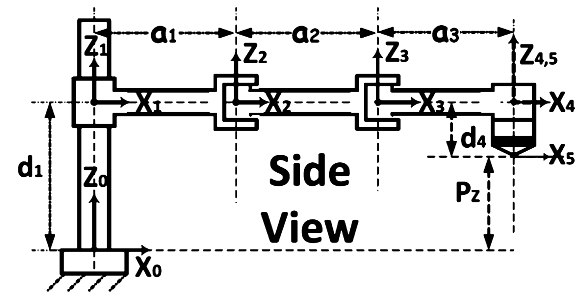

Fig. 5. Side view of the robotic arm [109,110].

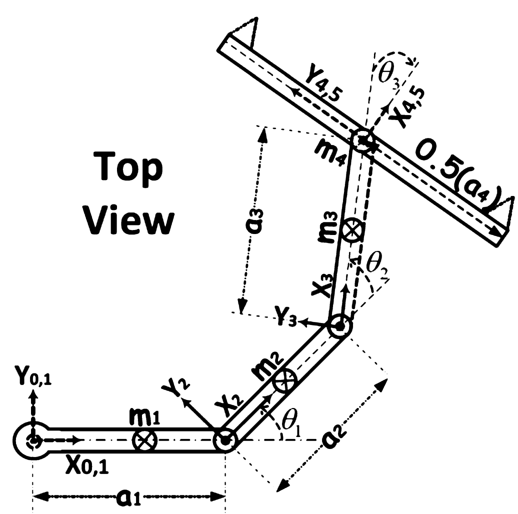

Fig. 6. Top view of the robotic arm [109,110].

(RRR) robot manipulator. The results demonstrated that SVSF increased the accuracy of the state trajectory accuracy by 30% over the EKF [107]. Also, Al-Shabi implemented the UK-SVSF to estimate the states of a PRRR robotic [108–111]. The results in these studies reveal that in the presence of both noise and uncertainty, UK-SVSF has the best performance as it can overcome the limitations in stability and sensitivity to the noise. Also, a new version of the UK-SVSF was applied to the same application and its results were compared to the previous version of UK-SVSF, UKF and SVSF. The new version of the UK-SVSF maintained improved results in calculating the RMSE when large amount of noise was injected to the system.

The SVSF has also been used for signal processing and state estimation in electro-mechanical systems and quadrotors [75,112]. In [75], the CK-SVSF method was utilized on a quadrotor controller. The results demonstrated that the CK-SVSF was more accurate, reliable, and stable over the standard filters (CKF and SVSF). The reduced form of the SVSF and EKF known respectively as RSVSF and REKF were applied on deep learning estimation with nine experiments using five different datasets with dissimilar network design [113]. These filters were applied to perform estimation and training of the large number of the neural networks. It was concluded that the RSVSF was preferable in all datasets compared to the REKF. In [114], SVSF was used as a technique to estimate the instantaneous feedback power and negative sequence in the direct power control (DPC) application. By the use of the SVSF, the number of sensors required in this application reduced to 2 instead of 6 sensors. Also, the results reveal that the SVSF has better performance compared to the KF due to its simplicity in its formulation while being accurate in the estimation of the Active Power (AP) and Reactive Power (RP) of the Positive Sequence (PS) components in addition to the Negative Sequence (NS) estimation. SVSF and its variants (EK-SVSF and UK-SVSF) were applied on an experimental case study for enhanced Partial Discharge (PD) localization [115]. Partial discharge is known as the sudden break down in power transformers due to aging or abnormal electrical, mechanical and thermal stresses [115]. Five different estimation techniques were used and compared for PD localization: EKF, UKF, SVSF, EK-SVSF and UK-SVSF. The results revealed that the UK-SVSF has superior performance over other filters as it is robust to the model uncertainty while maintaining the UKF optimality. The filter was reported to have less complexity in its formulation through eliminating the need for the Jacobian linearization.

Table 1
Parameters for the robotic arm [109].

m_1	21.5 kg	a_1	0.25 cm	I_1	1.04 kg m^2
m_2	16 kg	a_2	1.2 cm	I_2	13 kg m^2
m_3	8.5 kg	a_3	0.8 cm	I_3	3.12 kg m^2
m_4	7.9 kg	a_4	1.2 cm	I_4	1 kg m^2
m_5	6.3 kg	a_5	0 cm	I_5	0.84 kg m^2

4. Case study: robotic manipulator

In this paper, a robotic arm manipulator is used to study the performance of five different filtering strategies, namely: UKF, CKF, SVSF, UK-SVSF, and CK-SVSF. The performance of these methods will be summarized and compared based on root mean squared error (RMSE).

4.1. Dynamics of the robotic arm

A 4-DOF robotic arm (one prismatic and three revolute joints; PRRR) was selected for study and is shown in Figs. 5 and 6, where the system parameters are defined in Table 1.

The dynamic model of this robot can be described as:

$$\begin{bmatrix} F_z \\ \tau_1 \\ \tau_2 \\ \tau_3 \end{bmatrix} = \begin{bmatrix} m_T & 0 & 0 & 0 \\ 0 & A_1 & A_4 & A_5 \\ 0 & A_4 & A_2 & A_6 \\ 0 & A_5 & A_6 & A_3 \end{bmatrix} \ddot{\Theta} + \begin{bmatrix} 0 \\ A_7 \\ A_8 \\ 0 \end{bmatrix} + \begin{bmatrix} -gm_T \\ 0 \\ 0 \\ 0 \end{bmatrix} \tag{113}$$

where, $\Theta = [d_1\ \theta_1\ \theta_2\ \theta_3]$, d_i is the ith-link offset, and θ_i is the ith-joint. The values of A_1 to A_8 can be calculated as [109]:

$$A_1 = \begin{bmatrix} \frac{m_2 a_2^2}{4} + m_3[a_2^2 + \frac{a_3^2}{4} + a_2 a_3 c_2] \\ +(m_4 + m_5)[a_2^2 + a_3^2 + 2a_2 a_3 c_2] \\ +(I_{ZZ2} + I_{ZZ3} + I_{ZZ4} + I_{ZZ5}) \end{bmatrix} \tag{114}$$

$$A_2 = \frac{1}{4} m_3 a_3^2 + (m_4 + m_5) a_3^2 + (I_{ZZ3} + I_{ZZ4} + I_{ZZ5}) \tag{115}$$

$$A_3 = A_5 = A_6 = [I_{ZZ4} + I_{ZZ5}] \tag{116}$$

$$A_4 = \begin{bmatrix} m_3[\frac{a_3^2}{2} + a_2 a_3 c_2] \\ +(I_{ZZ3} + I_{ZZ4} + I_{ZZ5}) \\ +2(m_4 + m_5)[a_3^2 + a_2 a_3 c_2] \end{bmatrix} \tag{117}$$

$$A_7 = -\begin{bmatrix} (m_3 + 2m_4 + 2m_5)\dot{\theta}_1 \dot{\theta}_2 \\ +\frac{1}{2}(m_3 + 2m_4 + 2m_5)\dot{\theta}_1^2 \end{bmatrix} a_2 a_3 s_2 \tag{118}$$

$$A_8 = -\begin{bmatrix} 2(m_3 + m_4 + m_5)\dot{\theta}_1 \dot{\theta}_2 \\ +\frac{1}{2}(m_3 + 2m_4 + 2m_5)\dot{\theta}_1^2 \end{bmatrix} a_2 a_3 s_2 \tag{119}$$

Table 2
Testing configurations.

Configuration	Measurements	V_{max}	W_{max}	Configuration	Measurements	V_{max}	W_{max}
1	Full	10^{-10}	10^{-6}	17	Partial	10^{-10}	10^{-6}
2	Full	10^{-4}	10^{-6}	18	Partial	10^{-4}	10^{-6}
3	Full	10^{-3}	10^{-6}	19	Partial	10^{-3}	10^{-6}
4	Full	10^{-1}	10^{-6}	20	Partial	10^{-1}	10^{-6}
5	Full	10^{-10}	10^{-2}	21	Partial	10^{-10}	10^{-2}
6	Full	10^{-4}	10^{-2}	22	Partial	10^{-4}	10^{-2}
7	Full	10^{-3}	10^{-2}	23	Partial	10^{-3}	10^{-2}
8	Full	10^{-1}	10^{-2}	24	Partial	10^{-1}	10^{-2}
9	Full	10^{-10}	1	25	Partial	10^{-10}	1
10	Full	10^{-4}	1	26	Partial	10^{-4}	1
11	Full	10^{-3}	1	27	Partial	10^{-3}	1
12	Full	10^{-1}	1	28	Partial	10^{-1}	1
13	Full	10^{-10}	10^{2}	29	Partial	10^{-10}	10^{2}
14	Full	10^{-4}	10^{2}	30	Partial	10^{-4}	10^{2}
15	Full	10^{-3}	10^{2}	31	Partial	10^{-3}	10^{2}
16	Full	10^{-1}	10^{2}	32	Partial	10^{-1}	10^{2}

Table 3
The statistic of maximum absolute error.

Config.	States	MAE															
		Mean								Variance							
		NU SVSF	UN SVSF	NU NEW	UN NEW	NU OLD	UN OLD	NU UKF	UN UKF	NU SVSF	UN SVSF	NU NEW	UN NEW	NU OLD	UN OLD	NU UKF	UN UKF
3	x1	2E−04	2E−04	2E−04	2E−04	2E−04	1E−04	6E−01	6E−01	8E−09	5E−09	2E−09	2E−09	7E−09	3E−09	9E−19	9E−19
	x2	1E−02	1E−02	1E−02	1E−02	1E−02	1E−02	1E+00	1E+00	8E−07	5E−07	9E−07	2E−07	3E−08	2E−07	3E−17	3E−17
	x3	3E−04	4E−04	1E−04	2E−04	3E−04	3E−04	4E−01	1E+00	7E−09	1E−08	1E−09	2E−09	1E−08	5E−09	3E−19	2E−18
	x4	1E−02	4E−02	2E−02	5E−02	1E−02	3E−02	1E+00	2E+00	5E−06	3E−05	6E−07	6E−10	2E−06	1E−08	2E−17	1E−16
	x5	6E−04	6E−04	1E−04	5E−04	4E−04	3E−04	1E+00	2E+00	3E−09	2E−09	1E−09	6E−09	3E−09	1E−08	2E−18	9E−19
	x6	4E−02	9E−02	2E−02	4E−02	2E−02	4E−02	3E+00	3E+00	6E−06	8E−05	6E−07	5E−06	5E−06	6E−06	2E−17	9E−18
	x7	2E−04	6E−04	2E−04	2E−04	2E−04	3E−04	1E−01	7E−01	3E−09	6E−09	7E−10	2E−09	2E−09	6E−09	2E−17	2E−17
	x8	2E−02	7E−02	2E−02	3E−02	2E−02	4E−02	2E+00	1E+00	4E−33	5E−05	1E−06	7E−06	4E−33	1E−05	3E−16	4E−17
21	x1	3E−04	2E−04	2E−04	2E−04	2E−04	2E−04	1E+00	1E+00	2E−10	2E−10	5E−11	7E−12	9E−10	1E−10	2E−10	8E−11
	x2	1E−02	1E−02	1E−02	1E−02	1E−02	1E−02	3E+00	2E+00	3E−07	4E−07	1E−07	6E−07	4E−07	4E−07	6E−10	2E−10
	x3	3E−04	3E−04	3E−04	3E−04	3E−04	3E−04	1E+00	6E−01	1E−09	8E−09	7E−10	1E−09	3E−09	1E−08	2E−10	6E−11
	x4	2E−02	5E−02	2E−02	5E−02	2E−02	5E−02	2E+00	2E+00	4E−06	6E−05	2E−06	3E−05	4E−06	5E−05	1E−09	8E−12
	x5	2E−04	3E−04	2E−04	3E−04	3E−04	3E−04	3E−02	5E−02	6E−11	9E−09	3E−10	4E−10	2E−08	1E−08	2E−11	1E−13
	x6	2E−02	5E−02	2E−02	4E−02	2E−02	5E−02	5E−01	9E−01	7E−06	2E−04	5E−06	6E−05	2E−06	1E−04	1E−10	5E−11
	x7	2E−04	3E−04	1E−04	5E−04	2E−04	3E−04	2E+00	2E+00	8E−10	4E−08	7E−12	4E−08	5E−10	3E−08	2E−09	1E−09
	x8	2E−02	4E−02	2E−02	4E−02	2E−02	4E−02	5E+00	4E+00	7E−06	4E−05	8E−07	3E−05	7E−06	5E−05	7E−09	2E−06
29	x1	8E−02	7E−02	2E−04	2E−04	3E−02	1E+00	2E−01	1E+00	1E−05	9E−06	2E−10	1E−11	2E−08	9E−03	7E−05	9E−03
	x2	5E−01	5E−01	1E−02	1E−02	2E+00	4E+00	5E+00	2E+00	2E−04	1E−05	4E−07	9E−07	4E−06	5E−02	3E+00	2E−02
	x3	6E−02	6E−02	2E−04	3E−04	INF	5E−01	INF	INF	8E−06	1E−07	1E−09	1E−09	INF	2E−04	INF	INF
	x4	6E−01	1E+00	2E−02	5E−02	INF	5E+00	INF	INF	3E−04	5E−05	5E−06	6E−05	INF	6E−04	INF	INF
	x5	5E−02	4E−02	2E−04	3E−04	INF	1E+00	INF	INF	3E−05	3E−06	1E−09	4E−10	INF	7E−04	INF	INF
	x6	4E−01	6E−01	2E−02	5E−02	INF	7E+00	INF	INF	7E−04	2E−04	6E−06	1E−04	INF	3E−04	INF	INF
	x7	1E−01	1E−01	1E−04	4E−04	INF	7E+00	INF	INF	2E−03	1E−03	8E−12	5E−08	INF	3E−03	INF	INF
	x8	5E−01	9E−01	2E−02	4E−02	INF	9E+01	INF	INF	1E−02	3E−02	7E−06	6E−05	INF	1E−25	INF	INF

Table 4
The statistic of root mean squared error.

Config.	States	RMSE															
		Mean								Variance							
		NU SVSF	UN SVSF	NU NEW	UN NEW	NU OLD	UN OLD	NU UKF	UN UKF	NU SVSF	UN SVSF	NU NEW	UN NEW	NU OLD	UN OLD	NU UKF	UN UKF
3	x1	1E−03	1E−03	1E−03	1E−03	1E−03	8E−04	3E+00	3E+00	4E−07	2E−07	6E−08	6E−08	3E−07	1E−07	8E−18	9E−18
	x2	3E−02	3E−02	4E−02	4E−02	3E−02	3E−02	1E+01	9E+00	6E−06	3E−06	1E−06	2E−06	6E−06	4E−06	2E−16	3E−16
	x3	2E−03	1E−03	5E−04	9E−04	2E−03	2E−03	1E+00	5E+00	3E−07	2E−07	2E−08	5E−08	5E−07	1E−07	2E−18	2E−17
	x4	4E−02	1E−01	6E−02	1E−01	4E−02	9E−02	6E+00	2E+01	1E−05	1E−05	2E−06	4E−06	1E−05	9E−05	1E−16	5E−16
	x5	3E−03	2E−03	5E−04	2E−03	2E−03	2E−03	6E+00	7E+00	2E−07	2E−07	2E−08	4E−07	1E−07	4E−07	4E−17	1E−17
	x6	6E−02	1E−01	6E−02	1E−01	4E−02	8E−02	2E+01	2E+01	7E−06	8E−06	2E−06	8E−06	6E−06	3E−04	4E−16	2E−16
	x7	9E−04	1E−03	6E−04	7E−04	1E−03	1E−03	4E−01	4E+00	1E−07	5E−08	2E−08	3E−08	1E−07	2E−07	2E−17	3E−16
	x8	3E−02	8E−02	4E−02	9E−02	2E−02	8E−02	6E+00	1E+01	5E−06	6E−05	1E−06	1E−05	7E−06	7E−05	2E−15	4E−15
21	x1	1E−03	1E−03	1E−03	9E−04	9E−04	1E−03	7E+00	6E+00	2E−09	5E−09	9E−10	7E−09	3E−08	4E−09	3E−09	1E−09
	x2	5E−02	4E−02	5E−02	4E−02	4E−02	4E−02	2E+01	2E+01	6E−06	7E−06	5E−08	7E−06	3E−06	5E−06	5E−08	2E−08
	x3	1E−03	1E−03	1E−03	1E−03	2E−03	2E−03	5E+00	3E+00	3E−08	3E−07	2E−08	1E−08	1E−07	5E−07	2E−09	1E−09
	x4	7E−02	2E−01	7E−02	2E−01	7E−02	2E−01	1E+01	9E+00	4E−06	1E−04	5E−06	1E−04	3E−06	1E−04	4E−08	8E−09
	x5	1E−03	1E−03	1E−03	1E−03	1E−03	1E−03	2E−01	2E−01	7E−09	3E−07	2E−08	8E−09	6E−07	5E−07	2E−10	3E−10
	x6	8E−02	2E−01	7E−02	2E−01	8E−02	2E−01	2E+00	3E+00	4E−06	3E−03	8E−07	2E−03	2E−05	2E−03	8E−09	1E−09
	x7	9E−04	2E−03	8E−04	3E−03	7E−04	2E−03	1E+01	9E+00	2E−08	2E−06	1E−09	2E−06	1E−08	2E−06	3E−08	2E−08
	x8	4E−02	2E−01	4E−02	2E−01	5E−02	1E−01	4E+01	3E+01	3E−06	9E−04	4E−06	1E−03	3E−05	7E−04	4E−07	2E−07
29	x1	5E−01	5E−01	1E−03	9E−04	INF	6E+00	INF	INF	5E−04	4E−04	2E−09	5E−09	INF	2E−01	INF	INF
	x2	2E+00	2E+00	5E−02	4E−02	INF	3E+01	INF	INF	1E−02	5E−03	2E−07	9E−06	INF	2E+00	INF	INF
	x3	4E−01	2E−01	1E−03	1E−03	INF	2E+00	INF	INF	6E−04	1E−04	4E−08	2E−08	INF	1E−02	INF	INF
	x4	2E+00	3E+00	7E−02	2E−01	INF	2E+01	INF	INF	5E−03	1E−03	8E−06	2E−04	INF	3E−01	INF	INF
	x5	3E−01	3E−01	1E−03	1E−03	INF	8E+00	INF	INF	3E−03	6E−04	1E−07	2E−08	INF	1E−02	INF	INF
	x6	1E+00	1E+00	7E−02	2E−01	INF	3E+01	INF	INF	2E−02	4E−03	5E−06	2E−03	INF	2E−02	INF	INF
	x7	6E−01	6E−01	8E−04	3E−03	INF	5E+01	INF	INF	7E−02	6E−02	5E−09	3E−06	INF	5E−01	INF	INF
	x8	3E+00	4E+00	4E−02	2E−01	INF	2E+02	INF	INF	3E−01	4E−01	4E−06	1E−03	INF	2E−01	INF	INF

Table 5
The statistic of regression line slope.

Config.	States	Slope regression															
		Mean								Variance							
		NU SVSF	UN SVSF	NU NEW	UN NEW	NU OLD	UN OLD	NU UKF	UN UKF	NU SVSF	UN SVSF	NU NEW	UN NEW	NU OLD	UN OLD	NU UKF	UN UKF
3	x1	1E+00	1E+00	1E+00	1E+00	1E+00	1E+00	−4E−01	−2E−01	1E−07	1E−07	3E−08	3E−08	6E−08	4E−08	3E−18	4E−18
	x2	1E+00	1E+00	1E+00	1E+00	1E+00	1E+00	7E−03	1E−01	2E−06	2E−06	4E−07	4E−07	7E−07	1E−07	2E−17	2E−17
	x3	0E+00	0E+00	0E+00	0E+00	0E+00	0E+00	0E+00	0E+00	0E+00	0E+00	0E+00	0E+00	0E+00	0E+00	0E+00	0E+00
	x4	0E+00	0E+00	0E+00	0E+00	0E+00	0E+00	0E+00	0E+00	0E+00	0E+00	0E+00	0E+00	0E+00	0E+00	0E+00	0E+00
	x5	1E+00	1E+00	1E+00	1E+00	1E+00	1E+00	5E−01	3E−01	8E−09	8E−09	1E−09	2E−08	2E−08	2E−08	3E−19	8E−20
	x6	0E+00	0E+00	0E+00	0E+00	0E+00	0E+00	0E+00	0E+00	0E+00	0E+00	0E+00	0E+00	0E+00	0E+00	0E+00	0E+00
	x7	0E+00	0E+00	0E+00	0E+00	0E+00	0E+00	0E+00	0E+00	0E+00	0E+00	0E+00	0E+00	0E+00	0E+00	0E+00	0E+00
	x8	0E+00	0E+00	0E+00	0E+00	0E+00	0E+00	0E+00	0E+00	0E+00	0E+00	0E+00	0E+00	0E+00	0E+00	0E+00	0E+00
21	x1	1E+00	1E+00	1E+00	1E+00	1E+00	1E+00	4E+00	3E+00	1E−08	3E−09	7E−10	3E−10	7E−08	1E−09	1E−09	4E−10
	x2	1E+00	1E+00	1E+00	1E+00	1E+00	1E+00	2E+00	1E+00	6E−08	8E−08	1E−08	1E−08	1E−06	3E−08	3E−09	8E−10
	x3	0E+00	0E+00	0E+00	0E+00	0E+00	0E+00	0E+00	0E+00	0E+00	0E+00	0E+00	0E+00	0E+00	0E+00	0E+00	0E+00
	x4	0E+00	0E+00	0E+00	0E+00	0E+00	0E+00	0E+00	0E+00	0E+00	0E+00	0E+00	0E+00	0E+00	0E+00	0E+00	0E+00
	x5	1E+00	1E+00	1E+00	1E+00	1E+00	1E+00	1E+00	1E+00	4E−10	9E−09	9E−10	9E−10	1E−08	2E−08	3E−12	7E−12
	x6	0E+00	0E+00	0E+00	0E+00	0E+00	0E+00	0E+00	0E+00	0E+00	0E+00	0E+00	0E+00	0E+00	0E+00	0E+00	0E+00
	x7	0E+00	0E+00	0E+00	0E+00	0E+00	0E+00	0E+00	0E+00	0E+00	0E+00	0E+00	0E+00	0E+00	0E+00	0E+00	0E+00
	x8	0E+00	0E+00	0E+00	0E+00	0E+00	0E+00	0E+00	0E+00	0E+00	0E+00	0E+00	0E+00	0E+00	0E+00	0E+00	0E+00
29	x1	9E−01	9E−01	1E+00	1E+00	3E+01	−3E+00	7E+00	3E+00	3E−04	2E−04	2E−09	5E−10	3E−03	5E−02	6E−03	5E−02
	x2	1E+00	2E+00	1E+00	1E+00	1E+01	−4E+00	7E+00	1E+00	2E−03	6E−04	2E−08	9E−09	1E−03	1E−01	6E−01	9E−02
	x3	0E+00	0E+00	0E+00	0E+00	0E+00	0E+00	0E+00	0E+00	0E+00	0E+00	0E+00	0E+00	0E+00	0E+00	0E+00	0E+00
	x4	0E+00	0E+00	0E+00	0E+00	0E+00	0E+00	0E+00	0E+00	0E+00	0E+00	0E+00	0E+00	0E+00	0E+00	0E+00	0E+00
	x5	1E+00	1E+00	1E+00	1E+00	INF	2E−01	INF	INF	4E−05	1E−05	4E−09	1E−09	INF	1E−04	INF	INF
	x6	0E+00	0E+00	0E+00	0E+00	0E+00	0E+00	0E+00	0E+00	0E+00	0E+00	0E+00	0E+00	0E+00	0E+00	0E+00	0E+00
	x7	0E+00	0E+00	0E+00	0E+00	0E+00	0E+00	0E+00	0E+00	0E+00	0E+00	0E+00	0E+00	0E+00	0E+00	0E+00	0E+00
	x8	0E+00	0E+00	0E+00	0E+00	0E+00	0E+00	0E+00	0E+00	0E+00	0E+00	0E+00	0E+00	0E+00	0E+00	0E+00	0E+00

Table 6
The statistic of regression line bias.

Config.	States	Bias regression															
		Mean								Variance							
		NU SVSF	UN SVSF	NU NEW	UN NEW	NU OLD	UN OLD	NU UKF	UN UKF	NU SVSF	UN SVSF	NU NEW	UN NEW	NU OLD	UN OLD	NU UKF	UN UKF
3	x1	−2E−04	−1E−04	−2E−04	−2E−04	−2E−04	−9E−05	−3E−02	−3E−02	1E−08	9E−09	2E−09	2E−09	4E−09	7E−10	1E−20	1E−20
	x2	7E−04	1E−03	6E−04	7E−04	6E−04	1E−03	−3E−01	−3E−01	1E−06	1E−06	2E−07	2E−07	4E−07	9E−08	2E−18	2E−18
	x3	−4E−01	−4E−01	−4E−01	−4E−01	−4E−01	−4E−01	−5E−01	−9E−01	8E−09	2E−09	1E−09	3E−09	7E−09	2E−08	2E−20	1E−19
	x4	−7E−05	−1E−04	7E−07	1E−04	−5E−04	2E−04	−6E−01	−2E+00	1E−07	2E−08	1E−08	2E−08	4E−08	9E−08	8E−19	6E−18
	x5	0E+00	0E+00	0E+00	0E+00	0E+00	0E+00	0E+00	0E+00	0E+00	0E+00	0E+00	0E+00	0E+00	0E+00	0E+00	0E+00
	x6	1E−04	2E−04	−1E−05	−6E−04	3E−04	7E−05	−2E+00	−3E+00	9E−08	5E−08	1E−08	4E−08	2E−07	1E−07	5E−18	2E−18
	x7	−6E−01	−6E−01	−6E−01	−6E−01	−6E−01	−6E−01	−6E−01	−3E−01	5E−09	3E−09	9E−10	1E−09	5E−09	9E−09	3E−18	3E−18
	x8	3E−05	−1E−04	6E−06	1E−07	2E−04	−4E−05	−2E−01	1E+00	3E−08	2E−08	1E−08	2E−08	3E−08	7E−08	6E−17	5E−17
21	x1	2E−04	1E−04	9E−05	1E−04	5E−05	1E−04	1E−01	1E−01	1E−10	3E−10	7E−11	2E−10	6E−09	1E−10	2E−12	5E−13
	x2	4E−03	4E−03	4E−03	4E−03	3E−03	4E−03	1E+00	2E+00	2E−08	4E−08	8E−09	2E−08	7E−07	2E−08	3E−10	8E−11
	x3	−4E−01	−4E−01	−4E−01	−4E−01	−4E−01	−4E−01	3E−02	−5E−02	1E−10	9E−09	2E−10	2E−09	1E−08	2E−08	1E−11	1E−11
	x4	3E−04	2E−04	3E−04	1E−04	2E−04	2E−04	2E+00	9E−01	5E−09	7E−08	4E−11	8E−09	1E−07	8E−08	5E−10	2E−10
	x5	0E+00	0E+00	0E+00	0E+00	0E+00	0E+00	0E+00	0E+00	0E+00	0E+00	0E+00	0E+00	0E+00	0E+00	0E+00	0E+00
	x6	−8E−05	1E−04	−7E−05	1E−04	2E−04	1E−04	−3E−02	5E−02	5E−09	6E−08	1E−10	2E−09	6E−08	9E−08	1E−10	8E−12
	x7	−6E−01	−6E−01	−6E−01	−6E−01	−6E−01	−6E−01	5E−01	2E−01	1E−09	4E−08	2E−10	3E−08	2E−09	3E−08	3E−10	2E−10
	x8	−7E−05	−2E−04	−2E−04	−4E−04	−8E−07	−1E−04	4E+00	3E+00	7E−08	1E−07	4E−11	7E−08	2E−08	7E−08	5E−09	3E−09
29	x1	−4E−02	−4E−02	1E−04	1E−04	3E−03	1E−01	−6E−04	1E−01	3E−06	1E−06	1E−10	1E−10	2E−10	6E−05	6E−08	5E−05
	x2	−5E−01	−5E−01	4E−03	4E−03	8E−01	1E+00	−2E−02	2E+00	5E−04	2E−04	1E−08	1E−08	1E−06	8E−03	2E−02	8E−03
	x3	−4E−01	−4E−01	−4E−01	−4E−01	−INF	−4E−01	−INF	INF	8E−06	7E−06	7E−10	2E−09	INF	5E−04	INF	INF
	x4	−5E−02	−2E−02	3E−04	1E−04	INF	−6E−01	−INF	INF	1E−04	1E−04	2E−10	8E−09	INF	1E−02	INF	INF
	x5	0E+00	0E+00	0E+00	0E+00	0E+00	0E+00	0E+00	0E+00	0E+00	0E+00	0E+00	0E+00	0E+00	0E+00	0E+00	0E+00
	x6	−4E−02	−3E−02	−5E−05	1E−04	INF	−2E+00	INF	INF	7E−04	2E−04	2E−10	3E−09	INF	2E−03	INF	INF
	x7	−7E−01	−7E−01	−6E−01	−6E−01	−INF	5E+00	INF	INF	1E−03	9E−04	1E−09	3E−08	INF	7E−03	INF	INF
	x8	−9E−02	−1E−01	−2E−04	−3E−04	INF	9E+00	−INF	INF	1E−02	1E−02	2E−10	9E−08	INF	1E−01	INF	INF

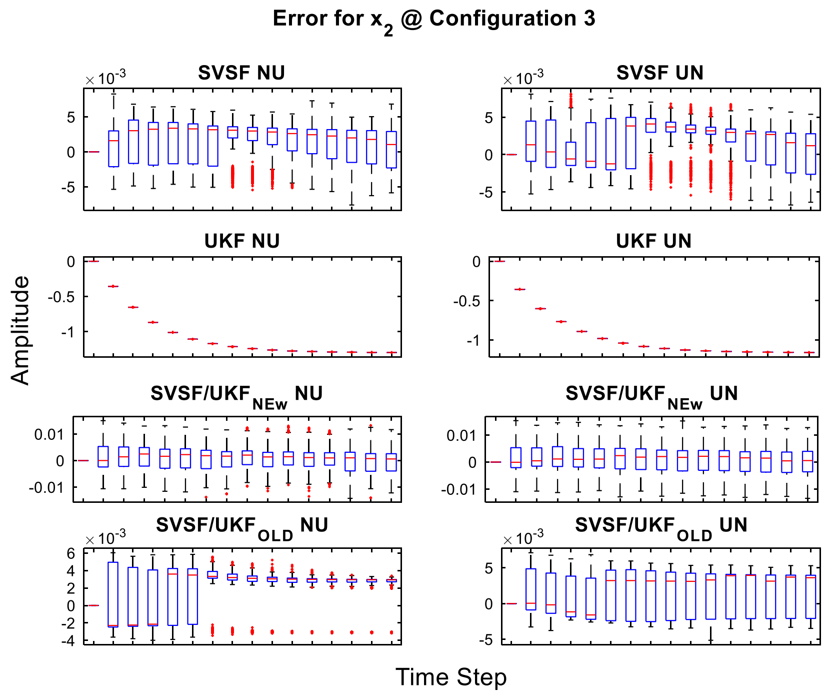

Fig. 7. Error in x_2 for the third configuration.

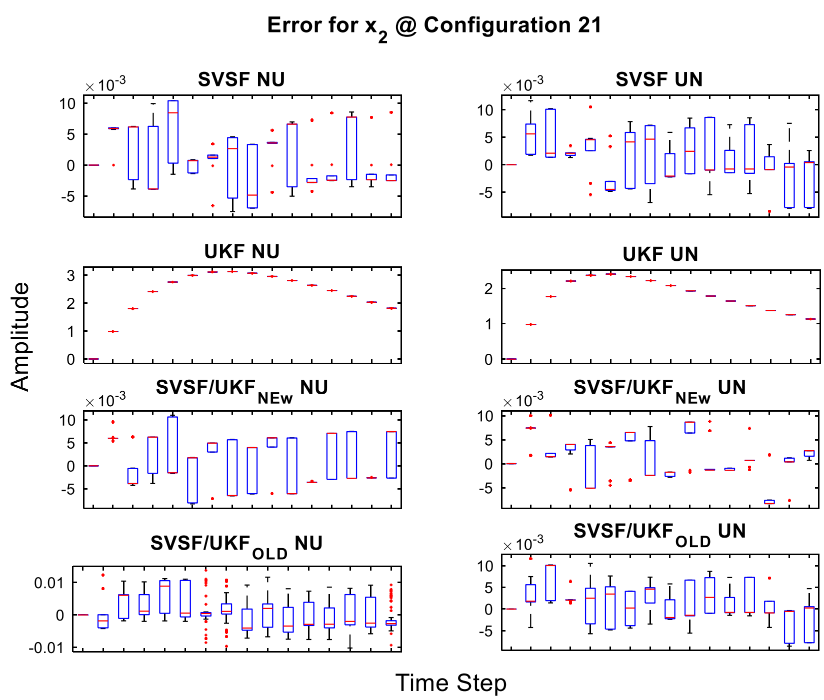

Fig. 8. Error in x_2 for the twenty first configuration.

where, a_i is the ith-link, m is the mass of each link, I is the moment of inertia, c_i and s_i represents the $\cos(\boldsymbol{\theta_i})$ and $\sin(\boldsymbol{\theta_i})$, respectively.

4.2. Summary of results

To compare the performance of the five filtering strategies, two different scenarios were considered: one without any uncertainty (NU), and the second with a very large amount of uncertainty (UN-around 50% of the system model). Two scenarios of measurements were considered: one with all states are measured, and the other one involved with only the variables ($\boldsymbol{d}$ and $\boldsymbol{\theta_i}$) are measured. Different levels of amplitude for the measurement noise were considered including $[10^{-10},\ 10^{-4},\ 10^{-3}$ and $10^{-1}]$. Same have been done for system noise with amplitudes of $[10^{-6},\ 10^{-2},\ 1,$ and $10^{2}]$. Note that the covariance matrices and the smooth boundary layers were set for the NU cases, where the covariance matrices were dependent on the noise characteristics and the boundary layer was tuned by trial-and-error. These considerations led to 32 configurations. These are summarized in Table 2.

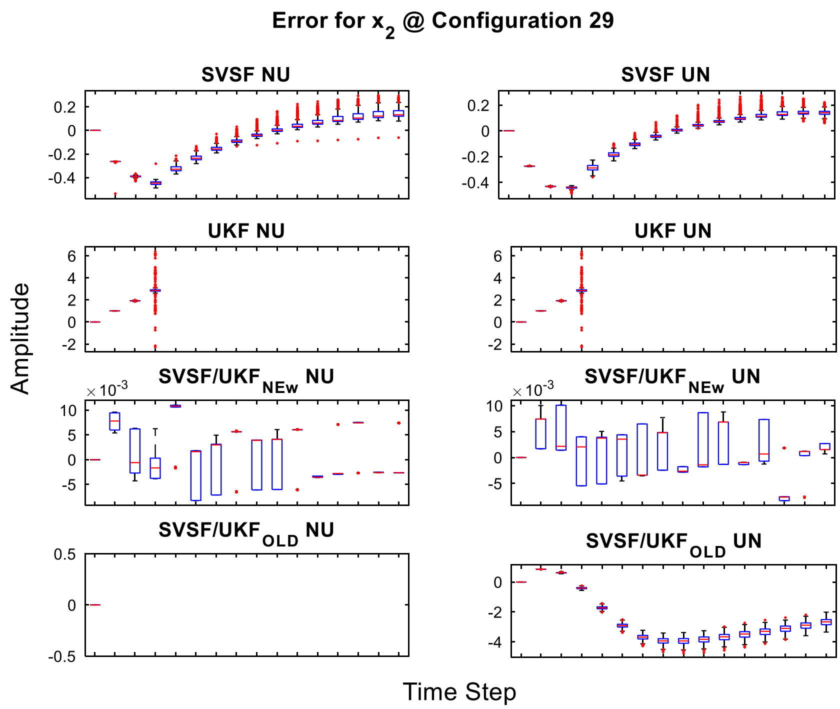

Fig. 9. Error in x_2 for the twenty ninth configuration.

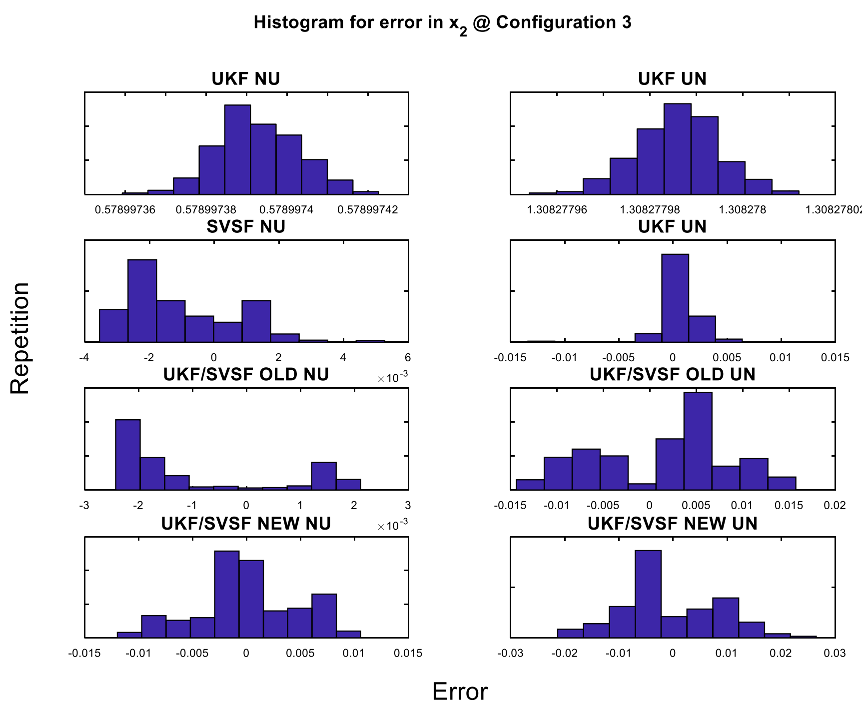

Fig. 10. The histogram of the error in x_2 for the third configuration.

The simulations were conducted 10000 times for each configuration, and the Root mean squared error (RMSE) and maximum absolute error (MAE) of each filter have been calculated. These are then summarized by their averages and standard deviations. The results are large to be listed in this work; therefore, only three configurations are listed in Table 3, Table 4, Table 5 and Table 6, and are illustrated (just for the second state) in Figs. 7–12. The results can be summarized as follows:

- If all states were measured, then all filters have good performances. Modeling uncertainties did not have a huge effect on the results.
- Reducing the number of measured states made the system exposed to the modeling uncertainties. As expected, UKF failed first, followed by SVSF/UKF old. Even if the filter did not fail for some configuration, the mean of the error showed a biasness from zero value. On the other hand, SVSF, and SVSF/UKF new did not fail.

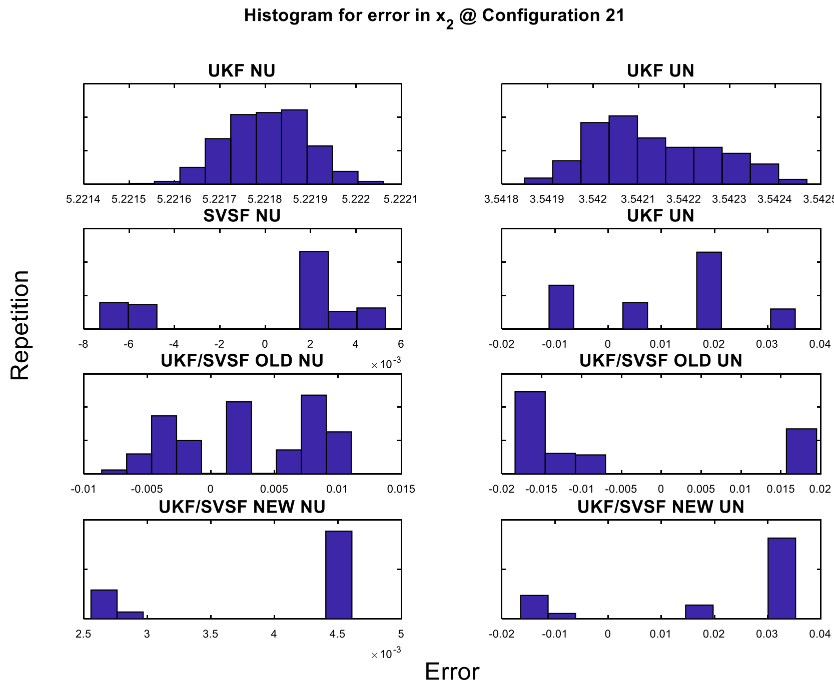

Fig. 11. The histogram of the error in x_2 for the twenty first configuration.

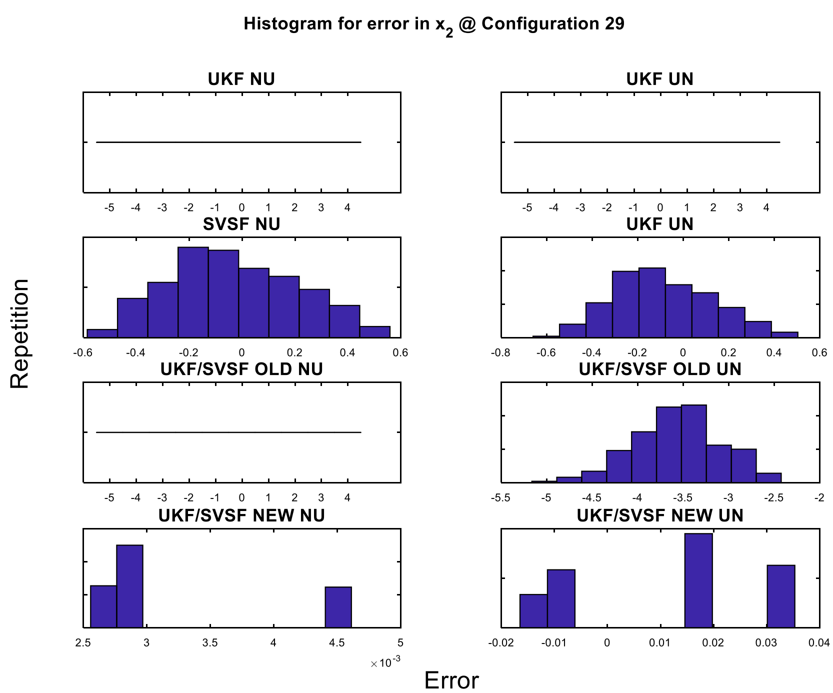

Fig. 12. The histogram of the error in x_2 for the twenty ninth configuration.

– Increasing the noise level made the results worse. Measurement noise had a higher effect than the system noise.

5. Conclusions

In this paper, a comprehensive review of the SVSF and its variants over the past 15 years was presented. The developments, applications and improvements of the SVSF in terms of robustness and optimality were investigated. The SVSF has been combined with a number of different filtering strategies to create new filters that maintain the robustness of the SVSF while benefiting from the accuracy of other strategies (e.g., KF for linear systems). Two main methods for combining the SVSF with other strategies include the use of a chattering function, and the use of the time-varying boundary layer. Two popular strategies that were created include the UK-SVSF and the CK-SVSF. These strategies were compared with the standard UKF, CKF, and SVSF through the use of a robotic manipulator. It was demonstrated that the UK-SVSF and CK-SVSF estimation strategies yielded the most accurate results and improved the robustness of the standard UKF and CKF. Future work related to the SVSF involves the application and development of artificial intelligence techniques and machine learning strategies such as deep and reinforcement learning.

Declaration of competing interest

The authors declare that they have no known competing financial interests or personal relationships that could have appeared to influence the work reported in this paper.

Acknowledgments

The work was supported in part by the Open Access Program from the American University of Sharjah. This article represents the opinions of the author(s) and does not mean to represent the position or opinions of the American University of Sharjah. The article was also supported by Natural Sciences and Engineering Research Council of Canada – Discovery Grant under the number RGPIN-2017-04087.

References

[1] Y. Bar-Shalom, X.R. Li, T. Kirubarajan, Estimation with Applications to Tracking and Navigation, Theory, Algorithms, and Software, John Wiley & Sons, New York, NY, USA, 2001.

[2] P.S. Maybeck, Stochastic Models, Estimation, and Control, Navtech Book & Software Store, Arlington, VA, 1999.

[3] Y. Ma, Q. Yu, I. Cohen, Target tracking with incomplete detection, Comput. Vis. Image Underst. 113 (4) (2009) 580–587.

[4] T. Quach, M. Farooq, Maximum likelihood track formation with the Viterbi algorithm, in: Proceedings of 1994 33rd IEEE Conference on Decision and Control, 2002, pp. 271–276.

[5] M. Shehab El Din, A.A. Hussein, M.F. Abdel-Hafez, Improved battery SOC estimation accuracy using a modified UKF with an adaptive cell model under real EV operating conditions, IEEE Trans. 4 (2) (2018) 408–417.

[6] H.W. Sorenson, Parameter Estimation: Principles and Problems, Ya Tung, Taipei, 1984.

[7] S. Geer, Least square estimation, in: Encyclopedia of Statistics in Behavioral Science, 2005.

[8] J.H. Donnelly, R.E. Shannon, Minimum mean-squared-error estimators for simulation experiments, Commun. ACM 24 (4) (1981) 253–259.

[9] T. Kailath, Lectures on Wiener and Kalman Filtering, 1981, pp. 1–143.

[10] T. Kailath, A view of three decades of linear filtering theory, IEEE Trans. Inf. Theory 20 (2) (1974) 146–181.

[11] S.A. Gadsden, S. Habibi, T. Kirubarajan, Kalman and smooth variable structure filters for robust estimation, IEEE Trans. Aerosp. Electron. Syst. 50 (2) (2014) 1038–1050.

[12] R.E. Kalman, A new approach to linear filtering and prediction problems, J. Basic Eng. 82 (1) (1960) 35.

[13] E.J. Lefferts, F.L. Markley, M.D. Shuster, Kalman filtering for spacecraft attitude estimation, J. Guid. Control Dyn. 5 (5) (2008) 417–429.

[14] R. Garcia, P. Pardal, H. Kuga, M. Zanardi, Nonlinear filtering for sequential spacecraft attitude estimation with real data: cubature Kalman filter, unscented Kalman filter and extended Kalman filter, Adv. Space Res. 63 (2) (2019) 1038–1050.

[15] J.K. Hlmann, S.J. Julier, Unscented filtering and nonlinear estimation, Proc. IEEE 92 (3) (2004) 401–422.

[16] S. Haykin, I. Arasaratnam, Cubature Kalman filters, IEEE Trans. Autom. Control 54 (6) (2009) 1254–1269.

[17] M. Negnevitsky, Artificial Intelligence: A Guide to Intelligent Systems, Systems, vol. 29, no. 1, 2nd edition, Pearson, Harlow, 2005.

[18] M.A.K. Jaradat, R. Langari, A hybrid intelligent system for fault detection and sensor fusion, Appl. Soft Comput. 9 (1) (2009) 415–422.

[19] M.A.K. Jaradat, M.F. Abdel-Hafez, Enhanced, delay dependent, intelligent fusion for ins/gps navigation system, IEEE Sens. J. 14 (5) (2014) 1545–1554.

[20] M.A.K. Jaradat, M.F. Abdel-Hafez, Non-linear autoregressive delay-dependent INS/GPS navigation system using neural networks, IEEE Sens. J. 17 (4) (2017) 1105–1115.

[21] M. Saadeddin, M.F. Abdel-Hafez, M.A. Jaradat, M.A. Jarrah, Optimization of intelligent-based approach for low-cost INS/GPS navigation system, in: 2013 International Conference on Unmanned Aircraft Systems (ICUAS), Atlanta, GA, USA, 28–31 May, 2013.

[22] K. Saadeddin, M.F. Abdel-Hafez, M.A. Jarrah, Estimating vehicle state by GPS/IMU fusion with vehicle dynamics, in: 2013 International Conference on Unmanned Aircraft Systems, ICUAS, Atlanta, GA, 2013, 2013, pp. 905–914.

[23] K. Saadeddin, M.F. Abdel-Hafez, M.A. Jaradat, M.A. Jarrah, Performance enhancement of low-cost, high-accuracy, state estimation for vehicle collision prevention system using ANFIS, Mech. Syst. Signal Process. 41 (1–2) (2013) 239–253.

[24] P.J. Escamilla-Ambrosio, N. Mort, Hybrid Kalman filter-fuzzy logic adaptive multisensor data fusion architectures, in: Proceedings of the IEEE Conference on Decision and Control, vol. 5, 2003, pp. 5215–5220.

[25] J.C. Chan, H. Ma, T.K. Saha, Hybrid method on signal de-noising and representation for online partial discharge monitoring of power transformers at substations, IET Sci. Meas. Technol. 9 (7) (2015) 890–899.

[26] R. Hussein, K.B. Shaban, A.H. El-Hag, Wavelet transform with histogram-based threshold estimation for online partial discharge signal denoising, IEEE Trans. Instrum. Meas. 64 (12) (2015) 3601–3614.

[27] J.L. Speyer, M.F. Abdel-Hafez, GPS measurement noise estimation in non-ideal environments, Navigation 55 (1) (2008) 55–66.

[28] A.-H. Mamoun, The autocovariance least-squares technique for GPS measurement noise estimation, IEEE Trans. Veh. Technol. 59 (2) (2010) 574–588.

[29] B.J. Odelson, M.R. Rajamani, J.B. Rawlings, A new autocovariance least-squares method for estimating noise covariances, Automatica 42 (2) (2006) 303–308.

[30] M.F. Abdel-Hafez, Detection of bias in GPS satellites' measurements: a probability ratio test formulation, IEEE Trans. Control Syst. Technol. 22 (3) (2014) 1166–1173.

[31] W.M.F. Al-Masri, M.F. Abdel-Hafez, A.H. El-Hag, A novel bias detection technique for partial discharge localization in oil insulation system, IEEE Trans. Instrum. Meas. 65 (2) (2016) 448–457.

[32] M.F. Abdel-Hafez, K. Saadeddin, M. Amin Jarrah, Constrained low-cost GPS/INS filter with encoder bias estimation for ground vehicles applications, Mech. Syst. Signal Process. 58 (2015) 285–297.

[33] A. Wadi, M. Abdel-Hafez, G.A. Husseini, Modeling and bias-robust estimation of the acoustic release of chemotherapeutics from liposomes, J. Biomed. Nanotechnol. 15 (1) (2019) 162–169.

[34] A. Wadi, M. Abdel-Hafez, G.A. Husseini, Identification of the uncertainty structure to estimate the acoustic release of chemotherapeutics from polymeric micelles, IEEE Trans. Nanobiosci. 16 (7) (2017) 609–617.

[35] W.M.F. Al-Masri, M.F. Abdel-Hafez, A.H. El-Hag, Toward high-accuracy estimation of partial discharge location, IEEE Trans. Instrum. Meas. 65 (9) (2016) 2145–2153.

[36] M. Shehab El Din, M.F. Abdel-Hafez, A.A. Hussein, Enhancement in Li-ion battery cell state-of-charge estimation under uncertain model statistics, IEEE Trans. Veh. Technol. 65 (6) (2016) 4608–4618.

[37] W.M.F. Al-Masri, M.F. Abdel-Hafez, A. El-Hag, A multi-hypothesis sequential probability test for partial discharges localization in power transformers, in: ISMA 2015 - 10th International Symposium on Mechatronics and Its Applications, 2015.

[38] M.F. Abdel-Hafez, On the GPS/IMU sensors' noise estimation for enhanced navigation integrity.pdf, Int. J. Math. Comput. Simul. 86 (2012) 101–117.

[39] L.L. Cam, Maximum likelihood: an introduction, Int. Stat. Rev. 58 (2) (1990) 153.

[40] M.A. Zagrobelny, J.B. Rawlings, Identifying the uncertainty structure using maximum likelihood estimation, in: Proceedings of the American Control Conference, vol. 2015, July, 2015, pp. 422–427.

[41] S. Habibi, The smooth variable structure filter, Proc. IEEE 95 (5) (2007) 1026–1059.

[42] V. Utkin, Variable structure systems with sliding modes, IEEE Trans. Autom. Control 22 (2) (2004) 212–222.

[43] V. Utkin, J. Guldner, J. Shi, Sliding Mode Control in Electromechanical Systems, CRC Press, Raton, 2009.

[44] J.-J.E. Slotine, J.K. Hedrick, E.A. Misawa, On sliding observers for nonlinear systems, J. Dyn. Syst. Meas. Control 109 (3) (2009) 245.

[45] B. Walcott, S. Zak, Observation of dynamical systems in the presence of bounded nonlinearities/uncertainties, in: 25th IEEE Conference on Decision and Control, 2008, pp. 961–966.

[46] C. Edwards, A comparison of sliding mode and unknown input observers for fault reconstruction, in: IEEE Conference on Decision and Control (CDC) (IEEE Cat. No. 04CH37601), 2004.

[47] J. He, J. Qiu, C. Zhang, C. Luo, Design of sliding mode observer for uncertain nonlinear systems, in: Proceedings of the World Congress on Intelligent Control and Automation (WCICA), 2008, pp. 1720–1723.

[48] S. Spurgeon, Sliding mode observers: a survey, Int. J. Syst. Sci. 39 (8) (2007) 751–764.

[49] Chee Pin Tan, C. Edwards, Sliding mode observers for reconstruction of simultaneous actuator and sensor faults, Int. J. Robust Nonlinear Control 13 (5) (2004) 1455–1460.

[50] D.G. Bates, C. Turner, Mathematical Methods for Robust and Nonlinear Control, Springer, Berlin, 2007.

[51] M. Al-Shabi, The General Toeplitz/Observability Smooth Variable Structure Filter, 2011.

[52] S.R. Habibi, R. Burton, The variable structure filter, J. Dyn. Syst. Meas. Control 125 (3) (2003) 287.

[53] S.A. Gadsden, H.H. Afshari, A review of smooth variable structure filters: recent advances in theory and applications, in: Advances in Theory and Applications, Dynamics, Vibration, and Control, vol. 4A, 2016, V04AT04A055.
[54] S.A. Gadsden, Smooth Variable Structure Filtering: Theory and Applications, 2011.
[55] S. Habibi, The extended variable structure filter, J. Dyn. Syst. Meas. Control 128 (2) (2006) 341.
[56] H. Afshari, S.A. Gadsden, S. Habibi, Gaussian filters for parameter and state estimation: a general review of theory and recent trends, Signal Process. 135 (2017) 218–238.
[57] M. Al-Shabi, S. Gadsden, S. Habibi, Kalman filtering strategies utilizing the chattering effects of the smooth variable structure filter, Signal Process. 93 (2) (2013) 420–431.
[58] H.H. Afshari, S.A. Gadsden, S. Habibi, A nonlinear second-order filtering strategy for state estimation of uncertain systems, Signal Process. 155 (2019) 182–192.
[59] H. Afshari, The 2nd-order smooth variable structure filter (2nd-SVSF) for state estimation: theory and applications, Handle Proxy, 01-Jun-2015, 2015.
[60] J.L. Crassidis, F.L. Markley, Predictive filtering for nonlinear systems, J. Guid. Control Dyn. 20 (3) (2008) 566–572.
[61] L. Cao, Y. Chen, Z. Zhang, H. Li, A.K. Misra, Predictive smooth variable structure filter for attitude synchronization estimation during satellite formation flying, IEEE Trans. Aerosp. Electron. Syst. 53 (3) (2017) 1375–1383.
[62] J.-J.E. Slotine, W. Li, Applied Nonlinear Control: An Introduction, Prentice-Hall, Englewood Cliffs, NJ, 1991.
[63] D. Lingaiah, Kalman Filtering: Theory and Practice Using MATLAB, 2nd ed., Book Review, vol. 19, John Wiley & Sons, Hoboken, NJ, 2003.
[64] S.A. Gadsden, M. Al-Shabi, T. Kirubarajan, Square-root formulation of the SVSF with applications to nonlinear target tracking problems, in: Signal Processing, Sensor/Information Fusion, and Target Recognition XXIV, vol. 9474, 2015, p. 947408.
[65] S.A. Gadsden, S.R. Habibi, A new robust filtering strategy for linear systems, J. Dyn. Syst. Meas. Control 135 (1) (2012) 014503.
[66] S.A. Gadsden, M. El Sayed, S.R. Habibi, Derivation of an optimal boundary layer width for the smooth variable structure filter, in: Proceedings of the 2011 American Control Conference, 2014, pp. 4922–4927.
[67] M. Al-Shabi, S. Habibi, New novel time-varying and robust smoothing boundary layer width for the smooth variable structure filter, in: 2013 9th International Symposium on Mechatronics and Its Applications, ISMA 2013, 2013.
[68] F. Outamazirt, L. Fu, Y. Lin, N. Abdelkrim, A new SINS/GPS sensor fusion scheme for UAV localization problem using nonlinear SVSF with covariance derivation and an adaptive boundary layer, Chin. J. Aeronaut. 29 (2) (2016) 424–440.
[69] S.A. Gadsden, S.R. Habibi, A new form of the smooth variable structure filter with a covariance derivation, in: Proceedings of the IEEE Conference on Decision and Control, 2010, pp. 7389–7394.
[70] W. Li, H. Gu, W. Su, Partitioned time-varying smooth variable structure filter for airport target tracking, in: 2016 CIE International Conference on Radar, RADAR 2016, 2017.
[71] S. Habibi, Parameter estimation using a combined variable structure and Kalman filtering approach, J. Dyn. Syst. Meas. Control 130 (5) (2008) 051004.
[72] R.V.D. Merwe, E. Wan, The unscented Kalman filter for nonlinear estimation, in: Proceedings of the IEEE 2000 Adaptive Systems for Signal Processing, Communications, and Control Symposium (Cat. No. 00EX373), 2000.
[73] S. Haykin, I. Arasaratnam, Cubature Kalman filters, IEEE Trans. Autom. Control 54 (6) (2009) 1254–1269.
[74] S. Gadsden, M. Al-Shabi, I. Arasaratnam, S. Habibi, Combined cubature Kalman and smooth variable structure filtering: a robust nonlinear estimation strategy, Signal Process. 96 (2014) 290–299.
[75] M. Al-Shabi, S.A. Gadsden, S.A. Wilkerson, The cubature smooth variable structure filter estimation strategy applied to a quadrotor controller, in: Signal Processing, Sensor/Information Fusion, and Target Recognition XXIV, vol. 9474, 2015, 94741I.
[76] L.A. Zadeh, Outline of a new approach to the analysis of complex systems and decision processes, IEEE Trans. Syst. Man Cybern. 1 (1) (1973) 28–44.
[77] Lee-Ryeok, A fuzzy-Kalman filtering strategy for state estimation, Handle Proxy 01-Jun-2004, 2004.
[78] S.A. Gadsden, M.A. Al-Shabi, S.R. Habibi, A fuzzy-smooth variable structure filtering strategy: for state and parameter estimation, in: 2013 IEEE Jordan Conf. Appl. Electr. Eng. Comput. Technol. AEECT 2013, 2013.
[79] R. Ahmed, M. El Sayed, S.A. Gadsden, J. Tjong, S. Habibi, Automotive internal-combustion-engine fault detection and classification using artificial neural network techniques, IEEE Trans. Veh. Technol. 64 (1) (2015) 21–33.
[80] R. Ahmed, M. El Sayed, S.A. Gadsden, J. Tjong, S. Habibi, Artificial neural network training utilizing the smooth variable structure filter estimation strategy, Neural Comput. Appl. 27 (3) (2016) 537–548.
[81] H. Afshari, S.A. Gadsden, S. Habibi, Robust fault diagnosis of an electro-hydrostatic actuator using the novel dynamic second-order SVSF and IMM strategy, Int. J. Fluid Power (2014) 181–191.
[82] S.A. Gadsden, S.R. Habibi, State estimation and fault detection of an electro-hydrostatic actuator, in: ASME/BATH 2014 Symposium on Fluid Power and Motion Control, 2014, V001T01A032.
[83] M. Al-Shabi, S. Habibi, Iterative smooth variable structure filter for parameter estimation, ISRN Signal Process. 2011 (1) (2011) 1–18.
[84] S.A. Gadsden, H.H. Afshari, S.R. Habibi, Development of a sliding mode controller and higher-order structure-based estimator, in: 2016 IEEE Transportation Electrification Conference and Expo, ITEC 2016, 2016.
[85] F. Demim, A. Nemra, H. Abdelkadri, A. Bazoula, K. Louadj, M. Hamerlain, SLAM problem for autonomous underwater vehicle using SVSF filter, in: 2018 25th International Conference on Systems, Signals and Image Processing, IWSSIP, 2018, pp. 1–5.
[86] A. Allam, A. Nemra, M. Hamerlain, Smooth variable structure filter VSLAM, IFAC-PapersOnLine 49 (15) (2016) 205–211.
[87] F. Demim, A. Nemra, K. Louadj, Robust SVSF-SLAM for unmanned vehicle in unknown environment, IFAC-PapersOnLine 49 (21) (2016) 386–394.
[88] F. Demim, A. Nemra, A. Boucheloukh, K. Louadj, M. Hamerlain, A. Bazoula, Robust SVSF-SLAM algorithm for unmanned vehicle in dynamic environment, in: 2018 International Conference on Signal, Image, Vision and Their Applications, SIVA, 2018, pp. 1–5.
[89] F. Demim, A. Nemra, A. Boucheloukh, E. Kobzili, M. Hamerlain, A. Bazoula, SLAM based on adaptive SVSF for cooperative unmanned vehicles in dynamic environment, IFAC-PapersOnLine 52 (8) (2019) 73–80.
[90] F. Demim, A. Boucheloukh, A. Nemra, E. Kobzili, M. Hamerlain, A. Bazoula, An adaptive SVSF-SLAM algorithm in dynamic environment for cooperative unmanned vehicles, IFAC-PapersOnLine 52 (15) (2019) 394–399.
[91] Y. Liu, C. Wang, A FastSLAM based on the smooth variable structure filter for UAVs, in: 2018 15th International Conference on Ubiquitous Robots, UR, 2018, pp. 591–596.
[92] W. Youn, S. Andrew Gadsden, Combined quaternion-based error state Kalman filtering and smooth variable structure filtering for robust attitude estimation, IEEE Access 7 (2019) 148989–149004.
[93] Y. Li, Y. He, G. Li, Y. Liu, Modified smooth variable structure filter for radar target tracking, in: 2019 International Radar Conference, RADAR, 2019, pp. 1–6.
[94] M. Attari, Z. Luo, S. Habibi, An SVSF-based generalized robust strategy for target tracking in clutter, IEEE Trans. Intell. Transp. Syst. 17 (5) (2016) 1381–1392.
[95] M. Attari, S.A. Gadsden, S.R. Habibi, A multi-target tracking formulation of SVSF with the joint probabilistic data association technique, in: 2013 American Control Conference, 2014, V002T26A002.
[96] S.A. Gadsden, D. Dunne, R. Tharmarasa, S.R. Habibi, T. Kirubarajan, Application of the smooth variable structure filter to a multi-target tracking problem, in: Signal Processing, Sensor Fusion, and Target Recognition XX, vol. 8050, 2011, p. 805009.
[97] S.A. Gadsden, D. Dunne, S.R. Habibi, T. Kirubarajan, Comparison of extended and unscented Kalman, particle, and smooth variable structure filters on a bearing-only target tracking problem, in: Signal and Data Processing of Small Targets 2009, vol. 7445, 2009, p. 74450B.
[98] S. Chen, Z. Shi, J. Ding, Application of the 2nd-order smooth variable structure filter algorithm for SINS initial alignment, in: 2017 Forum on Cooperative Positioning and Service, CPGPS 2017, 2017, pp. 43–49.
[99] H. Zhou, L. Xu, W. Chen, K. Guo, F. Shen, Z. Guo, A novel robust filtering strategy for systems with non-Gaussian noises, AEÜ, Int. J. Electron. Commun. 97 (2018) 154–164.
[100] S.A. Gadsden, A.S. Lee, Advances of the smooth variable structure filter: square-root and two-pass formulations, J. Appl. Remote Sens. 11 (1) (2017) 015018.
[101] S.A. Gadsden, M. Al-Shabi, T. Kirubarajan, Two-pass smoother based on the SVSF estimation strategy, in: Signal Processing, Sensor/Information Fusion, and Target Recognition XXIV, vol. 9474, 2015, p. 947409.
[102] S.R.H. Mohammed Farag, Mina Attari, S. Andrew Gadsden, Lithium-ion battery state of charge estimation using one state hysteresis model with nonlinear estimation strategies, Int. J. Chem. Mol. Nucl. Mater. Metall. Eng. 11 (3) (2017) 214–218.
[103] H.H. Afshari, M. Attari, R. Ahmed, A. Delbari, S. Habibi, T. Shoa, Reliable state of charge and state of health estimation using the smooth variable structure filter, Control Eng. Pract. 77 (2018) 1–14.
[104] M. Farag, M. Fleckenstein, S.R. Habibi, Li-ion battery SOC estimation using non-linear estimation strategies based on equivalent circuit models, SAE Tech. Pap. Ser. 1 (2014) 10–4271.
[105] A. Elnady, M. Al-Shabi, A.A. Adam, Novel filters based operational scheme for five-level diode-clamped inverters in microgrid, Front. Energy Res. 8 (2020) 11.
[106] R. Ahmed, S. Rahimifard, S. Habibi, Offline parameter identification and SOC estimation for new and aged electric vehicles batteries, in: 2019 IEEE Transportation Electrification Conference and Expo (ITEC), 2019, pp. 1–6.
[107] J. Goodman, J. Kim, A.S. Lee, S.A. Gadsden, M. Al-Shabi, A variable structure-based estimation strategy applied to an RRR robot system, J. Robot. Netw. Artif. Life 4 (2) (2017) 142.

[108] M. Al-Shabi, K.S. Hatamleh, The unscented smooth variable structure filter application into a robotic arm, in: Proceedings of the ASME 2014 International Mechanical Engineering Congress and Exposition. Volume 4B: Dynamics, Vibration, and Control, Montreal, Quebec, Canada, November 14–20, 2014, ASME, V04BT04A037.
[109] M. Al-Shabi, Sigma-point smooth variable structure filters applications into robotic arm, in: 2017 7th International Conference on Modeling, Simulation, and Applied Optimization, ICMSAO 2017, 2017.
[110] M. Al-Shabi, K.S. Hatamleh, The unscented smooth variable structure filter application into a robotic arm, in: 2015 IEEE 12th International Multi-Conference on Systems, Signals & Devices, SSD15, 2015, V04BT04A037.
[111] M. AlShabi, K.S. Hatamleh, S.A. Gadsden, B. Soudan, A. El-Nady, Robust nonlinear control and estimation of an PRRR robot system, Int. J. Robot. Automat. 34 (2019).
[112] S.A. Gadsden, T. Kirubarajan, Development of a variable structure-based fault detection and diagnosis strategy applied to an electromechanical system, in: Signal Processing, Sensor/Information Fusion, and Target Recognition XXVI, vol. 10200, 2017, p. 102001E.
[113] M. Ismail, M. Attari, S. Habibi, S. Ziada, Estimation theory and neural networks revisited: REKF and RSVSF as optimization techniques for deep-learning, Neural Netw. 108 (2018) 509–526.
[114] M. AlShabi, A. Elnady, Recursive smooth variable structure filter for estimation processes in direct power control scheme under balanced and unbalanced power grid, IEEE Syst. J. 14 (1) (2020) 971–982.
[115] M. Avzayesh, M.F. Abdel-Hafez, W. Al-Masri, M. AlShabi, A.H. El-Hag, A hybrid estimation-based technique for partial discharge localization, IEEE Trans. Instrum. Meas. (2020) 1.

Mohammad Avzayesh was born in 1994 in Evaz, Iran. He graduated from Salman Farsi Iranian High-School (UAE) in 2012. He received his B.S. degree in mechanical engineering from University of Sharjah (UAE) in 2017. He joined American University of Sharjah (UAE) as a graduate student and teaching assistant with the department of mechanical engineering. He received his M.S. degree in mechanical engineering from American University of Sharjah (UAE) in 2020. His current research interests include state estimation, sensor fusion and Artificial Intelligent.

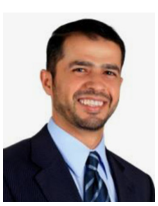

Mamoun Abdel-Hafez (M'14, SM'19) received the B.S. degree from the Jordan University of Science and Technology, Irbid, Jordan, in 1997, the M.S. degree from the University of Wisconsin, Milwaukee, WI, USA, in 1999, and the Ph.D. degree from the University of California at Los Angeles (UCLA), Los Angeles, CA, USA, in 2003, all in mechanical engineering. He served as a Post-Doctoral Research Associate with the Department of Mechanical and Aerospace Engineering, UCLA, in 2003, where he was involved in a research project on fault-tolerant autonomous multiple aircraft landing. He is currently a professor with the Department of Mechanical Engineering, American University of Sharjah, Sharjah, United Arab Emirates. His research interests include stochastic estimation, control systems, sensor fusion, and fault detection.

M. AlShabi is currently serving as an assistant professor in the Department of Mechanical & Nuclear Engineering at University of Sharjah/UAE. He obtained his BSc and MSc in Mechanical Engineering from Jordan University for Science and Technology/Jordan. He obtained his PhD in Mechanical Engineering/Mechatronics from McMaster University/Canada in 2011. His work involves in filters for state and parameter estimation, fault detection and diagnoses, and target tracking. He has several work in nonlinear control theory and sliding mode control applications. He is working in the field of artificial intelligence and their applications into robotics and mechatronics. His recent work involves in artificial neural network, fuzzy logic and metaheuristic techniques especially for parameter estimation and control.

S.A. Gadsden completed his Bachelors in Mechanical Engineering and Management (Business) at McMaster University. He completed his PhD in Mechanical Engineering at McMaster in the area of estimation theory with applications to mechatronics and aerospace systems. Dr. Gadsden worked as a postdoctoral researcher at the Centre for Mechatronics and Hybrid Technology (Hamilton, Ontario, Canada). He also worked as a Project Manager in the pharmaceutical industry (Apotex Inc.) for about three years. Before joining the University of Guelph, he was an Assistant Professor in the Department of Mechanical Engineering at the University of Maryland, Baltimore County (UMBC). Dr. Gadsden worked with a number of colleagues in NASA, the US Army Research Laboratory (ARL), US Department of Agriculture (USDA), National Institute of Standards and Technology (NIST), and the Maryland Department of the Environment (MDE). He is an elected Fellow of ASME, is a Senior Member of IEEE, and is a Professional Engineer of Ontario. Dr. Gadsden earned the 2019/2020 University Research Excellence Award for the College of Engineering and Physical Sciences based on his research activities at the University of Guelph. He is also a 2019 SPIE Rising Researcher award winner based on his work in intelligent estimation theory, and a 2018 Ontario Early Researcher award (ERA) winner based on his work in intelligent condition monitoring strategies. Dr. Gadsden was also awarded the 2019 University of Guelph Faculty Association (UGFA) Distinguished Professor Award for Excellence in Teaching in the College of Engineering and Physical Sciences.